Super-spreader hot-spots, mobility and lock-down effects on the dynamics of SIR epidemic models

Géza Ódor[1], Shengfeng Deng[2]
1. Research Institute for Technical Physics and Materials Science
2. Shaanxi Normal University
DSABNS Feb 7, 2024

Super-spreader hot-spots, mobility and lock-down effects on the dynamics of SIR epidemic models

Géza Ódor[1], Shengfeng Deng[2]
1. Research Institute for Technical Physics and Materials Science
2. Shaanxi Normal University
DSABNS Feb 7, 2024

1. Power-law vs Exponential behavior in Covid-19 data

Super-spreader hot-spots, mobility and lock-down effects on the dynamics of SIR epidemic models

Géza Ódor[1], Shengfeng Deng[2]
1. Research Institute for Technical Physics and Materials Science
2. Shaanxi Normal University
DSABNS Feb 7, 2024

1. Power-law vs Exponential behavior in Covid-19 data
2. The **S**usceptible **I**nfected **R**ecovered model

Super-spreader hot-spots, mobility and lock-down effects on the dynamics of SIR epidemic models

Géza Ódor[1], Shengfeng Deng[2]
1. Research Institute for Technical Physics and Materials Science
2. Shaanxi Normal University
DSABNS Feb 7, 2024

1. Power-law vs Exponential behavior in Covid-19 data
2. The **S**usceptible **I**nfected **R**ecovered model
3. Recent simulation results, suggesting slow epidemic decay

Super-spreader hot-spots, mobility and lock-down effects on the dynamics of SIR epidemic models

Géza Ódor[1], Shengfeng Deng[2]
1. Research Institute for Technical Physics and Materials Science
2. Shaanxi Normal University
DSABNS Feb 7, 2024

1. Power-law vs Exponential behavior in Covid-19 data
2. The **S**usceptible **I**nfected **R**ecovered model
3. Recent simulation results, suggesting slow epidemic decay
4. **H**ierarchical **M**odular **N**etworks

Super-spreader hot-spots, mobility and lock-down effects on the dynamics of SIR epidemic models

Géza Ódor[1], Shengfeng Deng[2]
1. Research Institute for Technical Physics and Materials Science
2. Shaanxi Normal University
DSABNS Feb 7, 2024

1. Power-law vs Exponential behavior in Covid-19 data
2. The **S**usceptible **I**nfected **R**ecovered model
3. Recent simulation results, suggesting slow epidemic decay
4. **H**ierarchical **M**odular **N**etworks
5. The simulation model used

Super-spreader hot-spots, mobility and lock-down effects on the dynamics of SIR epidemic models

Géza Ódor[1], Shengfeng Deng[2]
1. Research Institute for Technical Physics and Materials Science
2. Shaanxi Normal University
DSABNS Feb 7, 2024

1. Power-law vs Exponential behavior in Covid-19 data
2. The **S**usceptible **I**nfected **R**ecovered model
3. Recent simulation results, suggesting slow epidemic decay
4. **H**ierarchical **M**odular **N**etworks
5. The simulation model used
6. Results on **HMN**-s

Super-spreader hot-spots, mobility and lock-down effects on the dynamics of SIR epidemic models

Géza Ódor[1], Shengfeng Deng[2]
1. Research Institute for Technical Physics and Materials Science
2. Shaanxi Normal University
DSABNS Feb 7, 2024

1. Power-law vs Exponential behavior in Covid-19 data
2. The **S**usceptible **I**nfected **R**ecovered model
3. Recent simulation results, suggesting slow epidemic decay
4. **H**ierarchical **M**odular **N**etworks
5. The simulation model used
6. Results on **HMN**-s
7. The effect of mobility

Super-spreader hot-spots, mobility and lock-down effects on the dynamics of SIR epidemic models

Géza Ódor[1], Shengfeng Deng[2]
1. Research Institute for Technical Physics and Materials Science
2. Shaanxi Normal University
DSABNS Feb 7, 2024

1. Power-law vs Exponential behavior in Covid-19 data
2. The **S**usceptible **I**nfected **R**ecovered model
3. Recent simulation results, suggesting slow epidemic decay
4. **H**ierarchical **M**odular **N**etworks
5. The simulation model used
6. Results on **HMN**-s
7. The effect of mobility
8. The effect of a super-spreader hot spot

Super-spreader hot-spots, mobility and lock-down effects on the dynamics of SIR epidemic models

Géza Ódor[1], Shengfeng Deng[2]
1. Research Institute for Technical Physics and Materials Science
2. Shaanxi Normal University
DSABNS Feb 7, 2024

1. Power-law vs Exponential behavior in Covid-19 data
2. The **S**usceptible **I**nfected **R**ecovered model
3. Recent simulation results, suggesting slow epidemic decay
4. **H**ierarchical **M**odular **N**etworks
5. The simulation model used
6. Results on **HMN**-s
7. The effect of mobility
8. The effect of a super-spreader hot spot
   quenched disorder

Power vs. Exponential outbreak in various countries

COVID-19 epidemic data of more than 174 countries

(excluding China) in the period between 22 January and 28 March 2020

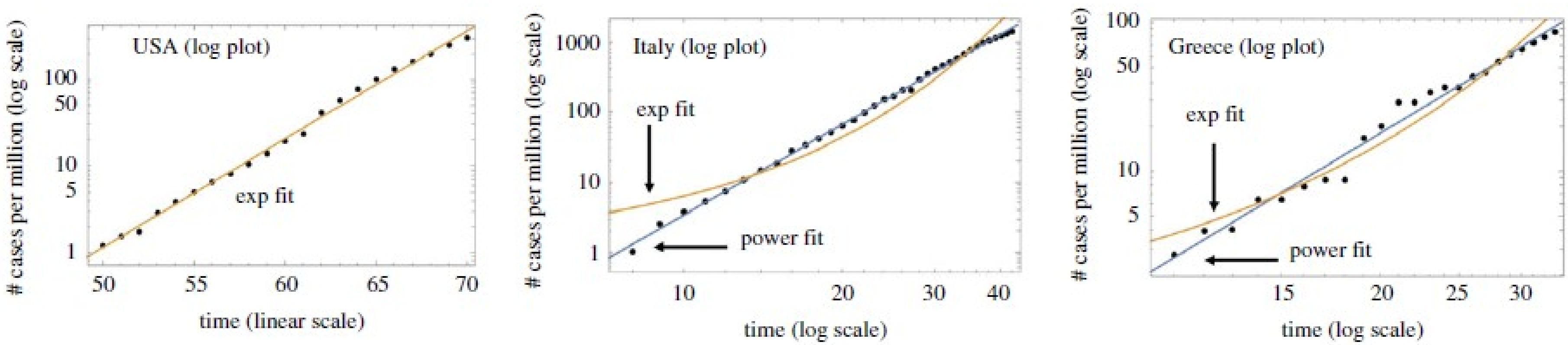

Figure 4. Examples of three error graph configurations. (*a*) USA, exponential; a log plot of the data is presented with the exponential fit. (*b*) Italy, power law; a log-log plot of the data is presented with the best fitting power law and exponential fits. (*c*) Greece, exponential-like; as in (*b*), a log-log plot is presented.

Komarova Natalia L., Schang Luis M. and Wodarz Dominik
2020 Patterns of the COVID-19 pandemic spread around the world: exponential versus power laws
J. R. Soc. Interface. ***17*** *20200518   http://doi.org/10.1098/rsif.2020.0518*

Power vs. Exponential outbreak in various countries

COVID-19 epidemic data of more than 174 countries
(excluding China) in the period between 22 January and 28 March 2020

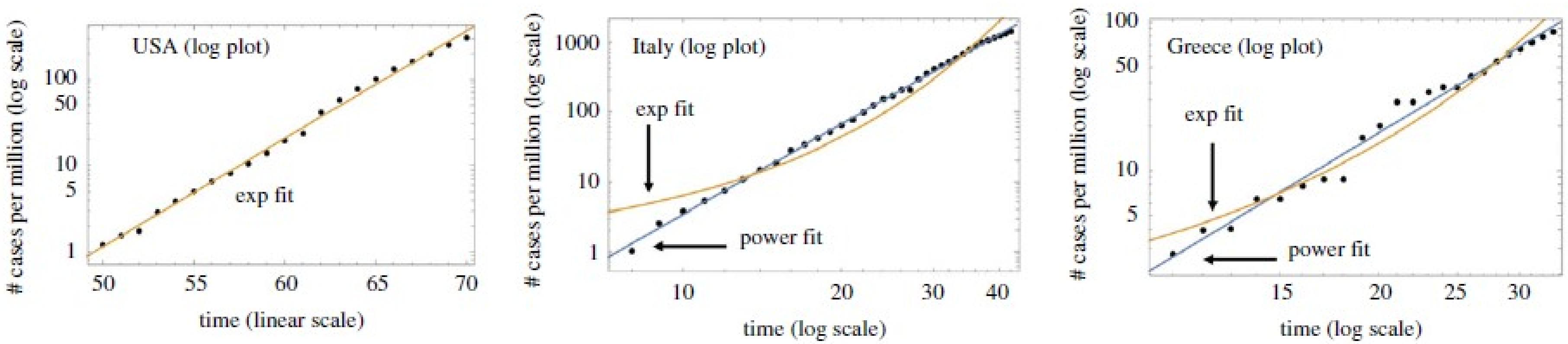

Figure 4. Examples of three error graph configurations. (*a*) USA, exponential; a log plot of the data is presented with the exponential fit. (*b*) Italy, power law; a log-log plot of the data is presented with the best fitting power law and exponential fits. (*c*) Greece, exponential-like; as in (*b*), a log-log plot is presented.

Komarova Natalia L., Schang Luis M. and Wodarz Dominik
2020 Patterns of the COVID-19 pandemic spread around the world: exponential versus power laws
J. R. Soc. Interface. ***17*** *20200518   http://doi.org/10.1098/rsif.2020.0518*

How can we understand different power-law exponents ?

Slow decay of infection in the inhomogeneous SIR model ?

Slow decay of infection in the inhomogeneous SIR model ?

Hidetsugu Sakaguchi and Yuta Nakao

Phys. Rev. E 103, 012301 (2021)

Slow decay of infection in the inhomogeneous SIR model ?

Hidetsugu Sakaguchi and Yuta Nakao

Phys. Rev. E 103, 012301 (2021)

SIR model in *1,2,3* dimensional lattices

Slow decay of infection in the inhomogeneous SIR model ?

Hidetsugu Sakaguchi and Yuta Nakao

Phys. Rev. E 103, 012301 (2021)

SIR model in *1,2,3* dimensional lattices

Inhomogenous infection rates (β_i)

Slow decay of infection in the inhomogeneous SIR model ?

Hidetsugu Sakaguchi and Yuta Nakao

Phys. Rev. E 103, 012301 (2021)

SIR model in *1,2,3* dimensional lattices

Inhomogenous infection rates (β_i)

D_s, D_I diffusion rates

Slow decay of infection in the inhomogeneous SIR model ?

Hidetsugu Sakaguchi and Yuta Nakao
Phys. Rev. E 103, 012301 (2021)

SIR model in *1,2,3* dimensional lattices

Inhomogenous infection rates (β_i)

$D_{s,}$ D_I diffusion rates

Numerical integration of

$$\frac{dS_i}{dt} = -\beta_i S_i I_i + D_S(S_{i+1} - 2S_i + S_{i-1}),$$
$$\frac{dI_i}{dt} = \beta_i S_i I_i - \gamma I_i + D_I(I_{i+1} - 2I_i + I_{i-1}),$$

Slow decay of infection in the inhomogeneous SIR model ?

Hidetsugu Sakaguchi and Yuta Nakao

Phys. Rev. E 103, 012301 (2021)

SIR model in *1,2,3* dimensional lattices

Inhomogenous infection rates (β_i)

$D_{s,}$ D_I diffusion rates

Numerical integration of

$$\frac{dS_i}{dt} = -\beta_i S_i I_i + D_S(S_{i+1} - 2S_i + S_{i-1}),$$

$$\frac{dI_i}{dt} = \beta_i S_i I_i - \gamma I_i + D_I(I_{i+1} - 2I_i + I_{i-1}),$$

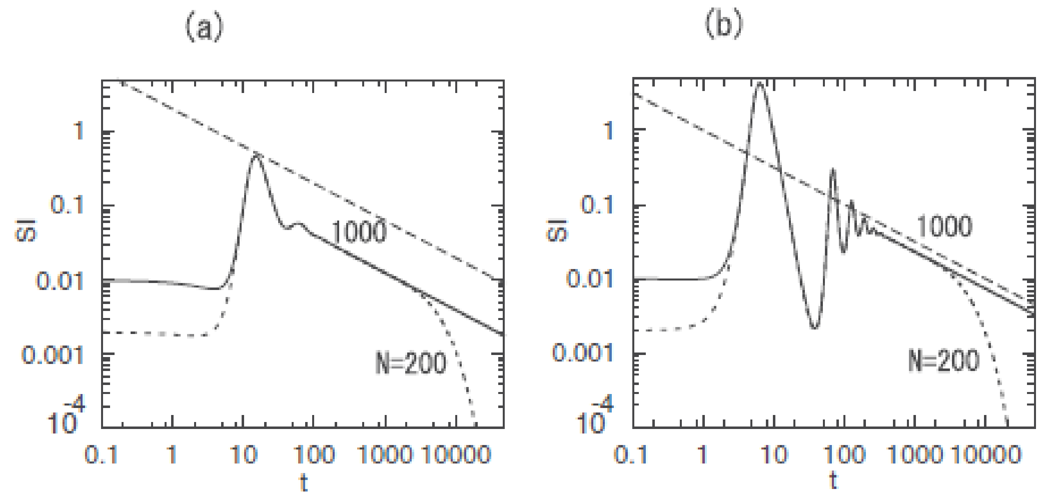

FIG. 2. (a) Time evolutions of $SI = \sum_{i=1}^{N} I_i$ for $N = 1000$ (solid line) and $N = 200$ (dotted line) at $D_S = 1$, $D_I = 1$, and $\gamma = 1$ in the double-logarithmic scale. The infection rate is $\beta_i = \beta_o = 0.9$ for $i \neq N/2$ and $\beta_i = 3$ at $i = N/2$. The straight dashed line denotes a power law of $1/t^{1/2}$. (b) Time evolutions of $SI = \sum_{i=1}^{N} I_i$ for $N = 1000$ (solid line) and $N = 200$ (dotted line) in the double-logarithmic scale. The infection rate is $\beta_i = 3$ for $N/2 - 7 \leqslant i \leqslant N/2 + 7$ and $\beta_0 = 0.9$ for the other region. Other parameters are the same as in Fig. 2(a).

Slow decay of infection in the inhomogeneous SIR model ?

Hidetsugu Sakaguchi and Yuta Nakao
Phys. Rev. E 103, 012301 (2021)

SIR model in *1,2,3* dimensional lattices

Inhomogenous infection rates (β_i)

$D_{s,}\ D_I$ diffusion rates

Numerical integration of

$$\frac{dS_i}{dt} = -\beta_i S_i I_i + D_S(S_{i+1} - 2S_i + S_{i-1}),$$

$$\frac{dI_i}{dt} = \beta_i S_i I_i - \gamma I_i + D_I(I_{i+1} - 2I_i + I_{i-1}),$$

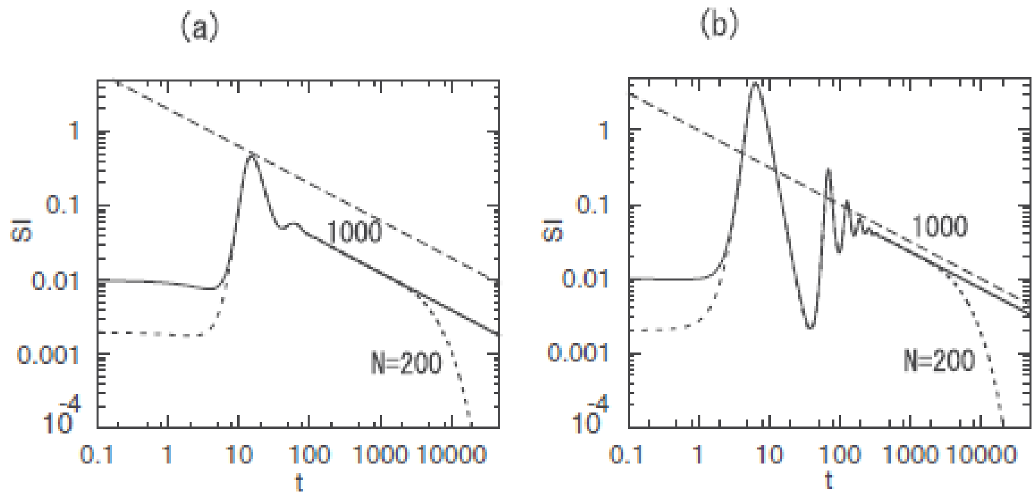

FIG. 2. (a) Time evolutions of $SI = \sum_{i=1}^{N} I_i$ for $N = 1000$ (solid line) and $N = 200$ (dotted line) at $D_S = 1$, $D_I = 1$, and $\gamma = 1$ in the double-logarithmic scale. The infection rate is $\beta_i = \beta_o = 0.9$ for $i \neq N/2$ and $\beta_i = 3$ at $i = N/2$. The straight dashed line denotes a power law of $1/t^{1/2}$. (b) Time evolutions of $SI = \sum_{i=1}^{N} I_i$ for $N = 1000$ (solid line) and $N = 200$ (dotted line) in the double-logarithmic scale. The infection rate is $\beta_i = 3$ for $N/2 - 7 \leqslant i \leqslant N/2 + 7$ and $\beta_0 = 0.9$ for the other region. Other parameters are the same as in Fig. 2(a).

Griffiths Phase behavior is suggested but where are the rare regions, with exponentially long lifetimes ?

Hierarchical, modular networks to model society with containment

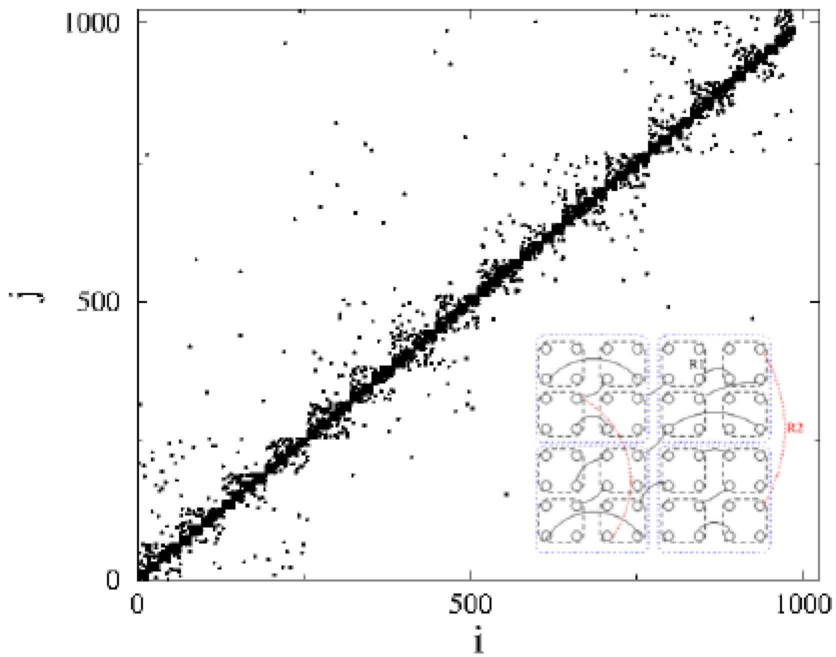

Hierarchical, modular networks to model society with containment

Embed network in *2d substrate*, modules of decreasing sizes recursively (continents, countries, cities, families)

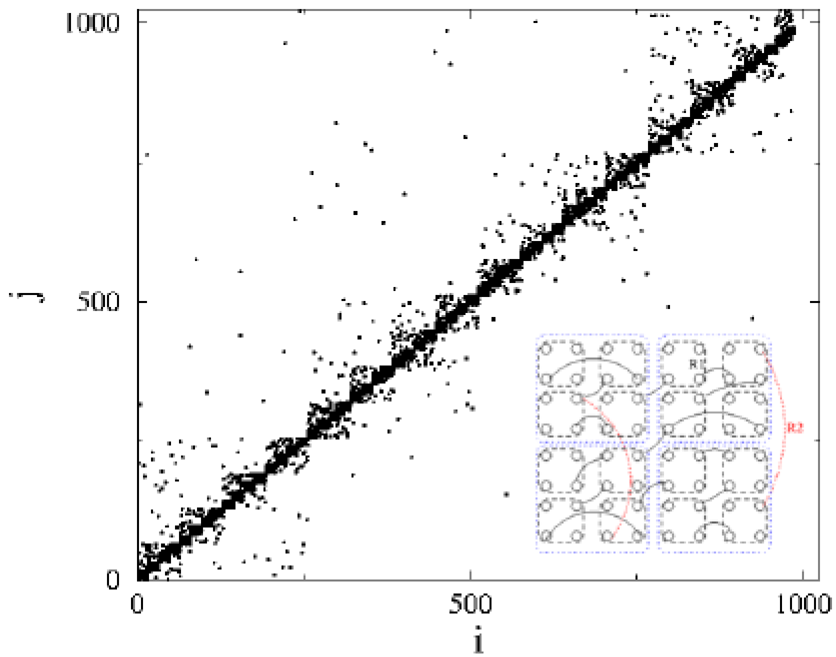

Hierarchical, modular networks to model society with containment

Embed network in *2d substrate*, modules of decreasing sizes recursively (continents, countries, cities, families)

Connect nodes with links on levels ($l=0, .., l_m$) with decreasing probabilities

$$p_l \sim \boldsymbol{b} \quad (1/2)^{\boldsymbol{s}\, \boldsymbol{l}}$$

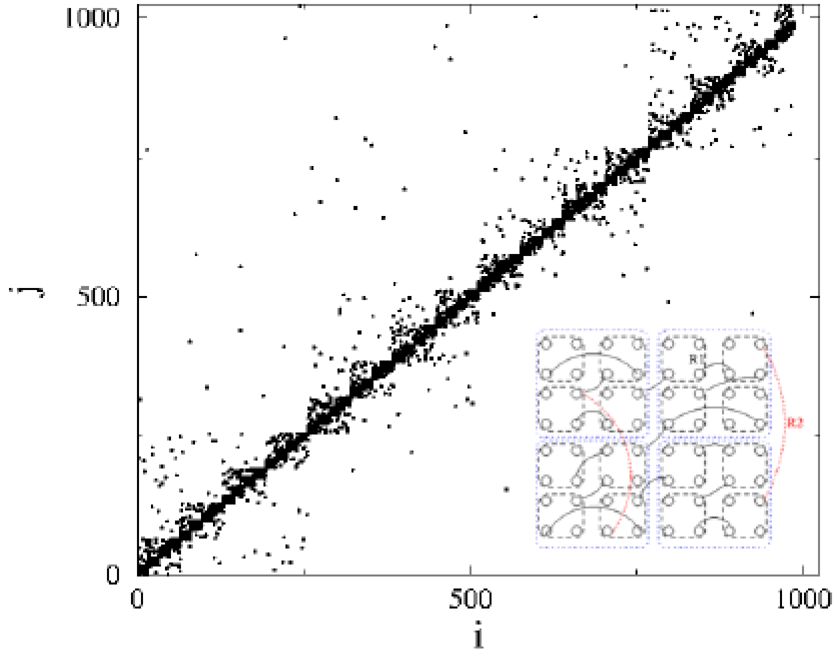

Hierarchical, modular networks to model society with containment

Embed network in *2d substrate*, modules of decreasing sizes recursively (continents, countries, cities, families)

Connect nodes with links on levels ($l=0, .., l_m$) with decreasing probabilities

$$p_l \sim \boldsymbol{b} \quad (1/2)^{\boldsymbol{s}\,\boldsymbol{l}}$$

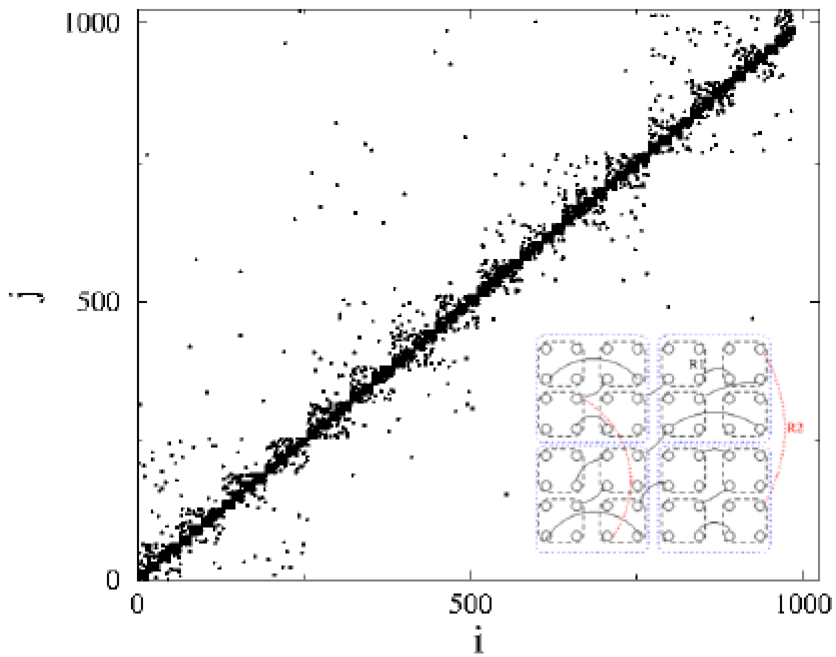

Use ***s*** *to control decay law and* ***b*** *to control <k>*

Hierarchical, modular networks to model society with containment

Embed network in *2d substrate*, modules of decreasing sizes recursively (continents, countries, cities, families)

Connect nodes with links on levels ($l=0, .., l_m$) with decreasing probabilities

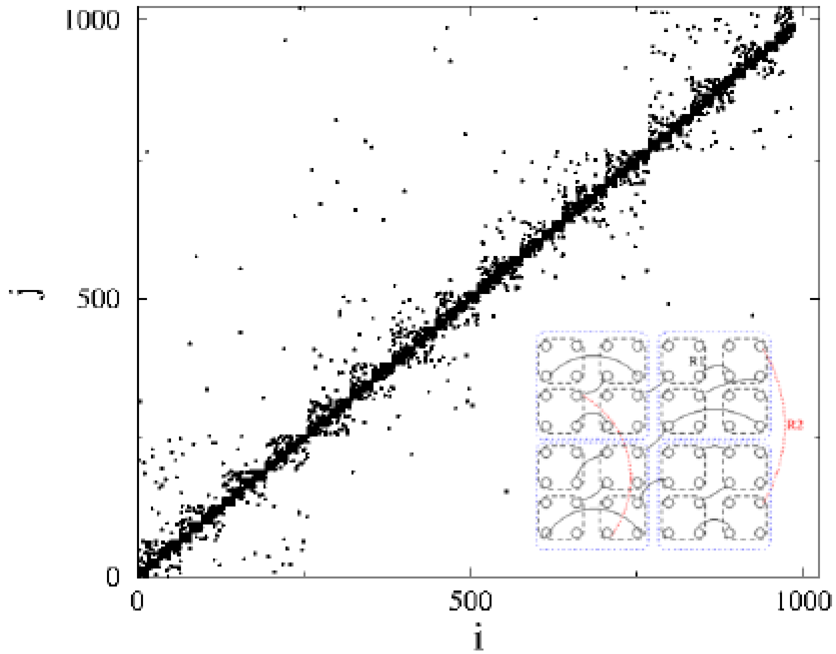

$$p_l \sim \boldsymbol{b} \quad (1/2)^{\boldsymbol{s}\, l}$$

*Use **s** to control decay law and **b** to control <k>*

Hierarchical, modular networks to model society with containment

Embed network in *2d substrate*, modules of decreasing sizes recursively (continents, countries, cities, families)

Connect nodes with links on levels ($l=0, .., l_m$) with decreasing probabilities

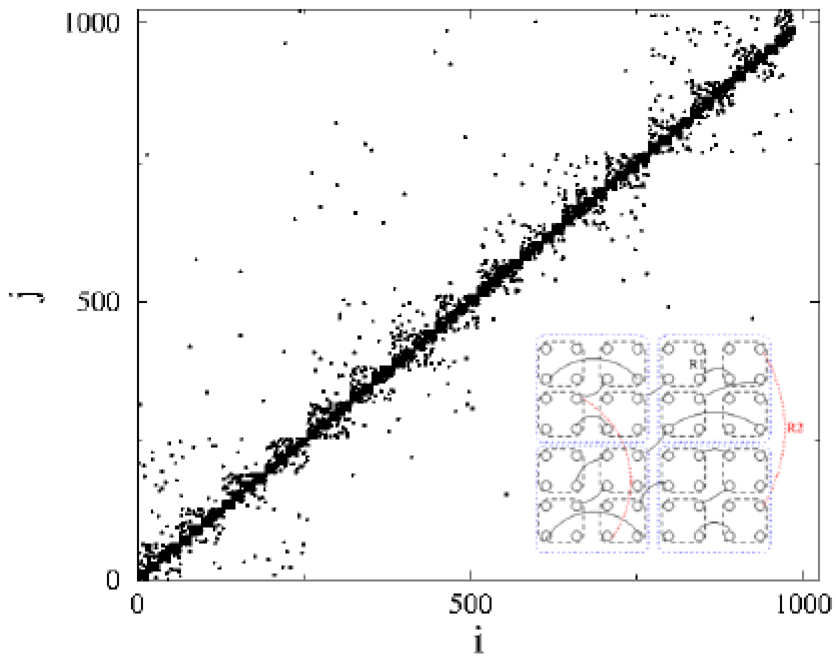

$$p_l \sim b \; (1/2)^{s\, l}$$

*Use **s** to control decay law and **b** to control <k>*

Hierarchical, modular networks to model society with containment

Embed network in *2d substrate*, modules of decreasing sizes recursively (continents, countries, cities, families)

Connect nodes with links on levels ($l=0, .., l_m$) with decreasing probabilities

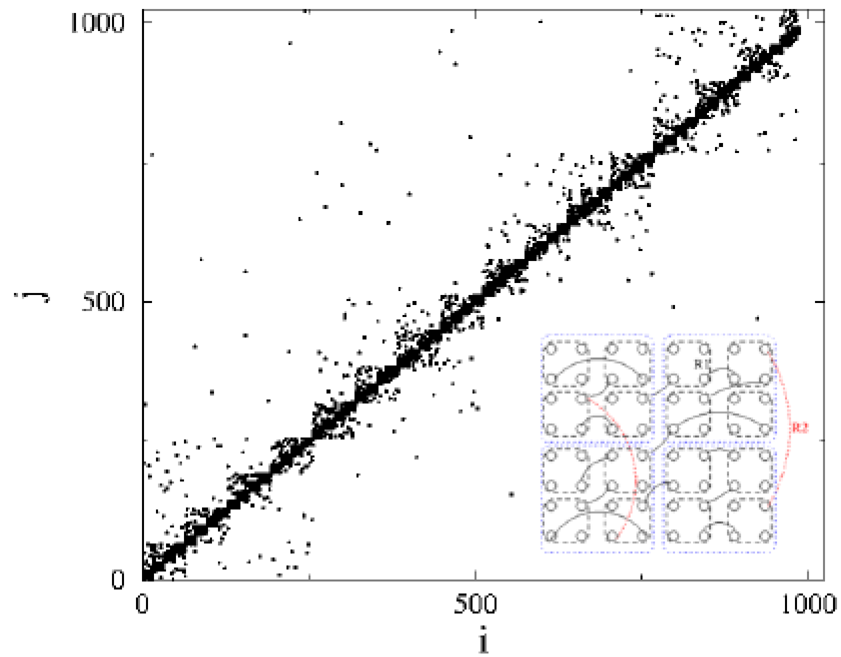

$$p_l \sim \boldsymbol{b}\ (½)^{s\,l}$$

*Use **s** to control decay law and **b** to control <k>*

www.nature.com/scientificreports

SCIENTIFIC REPORTS

SIS type!

OPEN

Griffiths phases and localization in hierarchical modular networks

Géza Ódor[1], Ronald Dickman[2] & Gergely Ódor[3]

Topological features

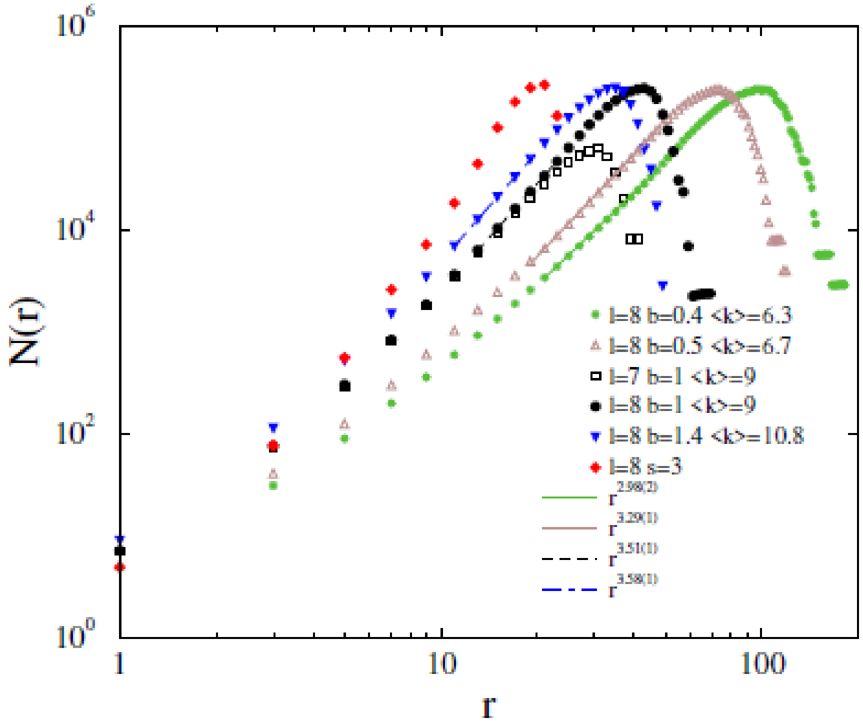

Topological features

Topological dimension : $N(r) \sim r^{d}$

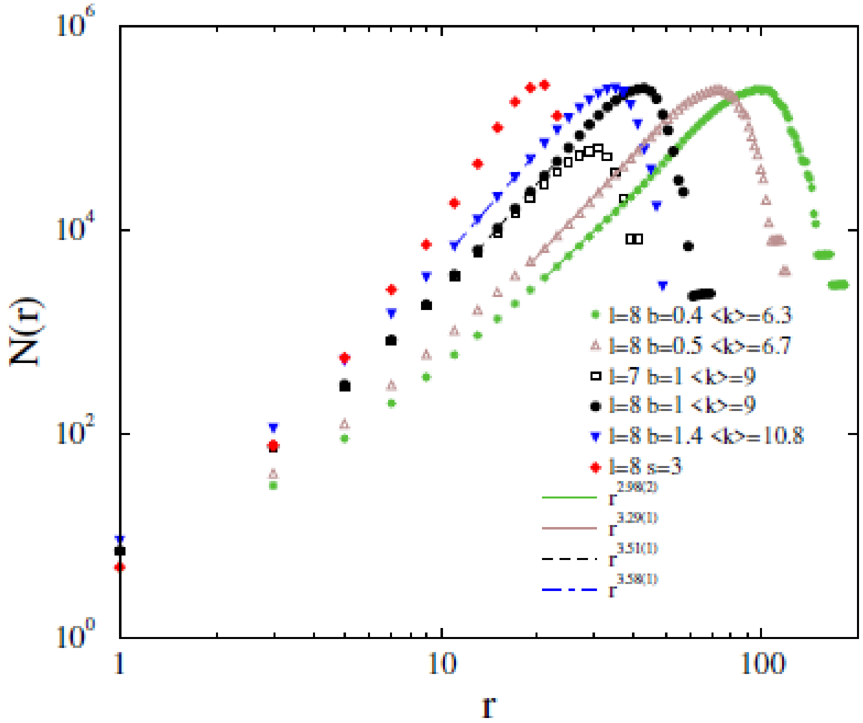

Topological features

Topological dimension : $N(r) \sim r^{d}$

Breadth-first search algorithm:

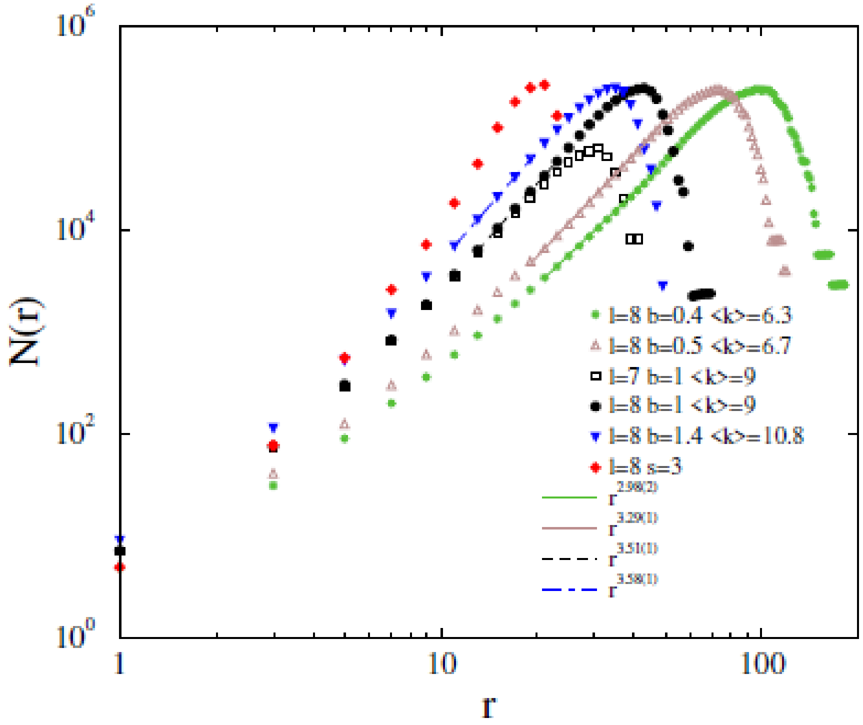

Topological features

Topological dimension : $N(r) \sim r^{\,d}$

Breadth-first search algorithm:

$s < 4$: $d \rightarrow \infty$ network

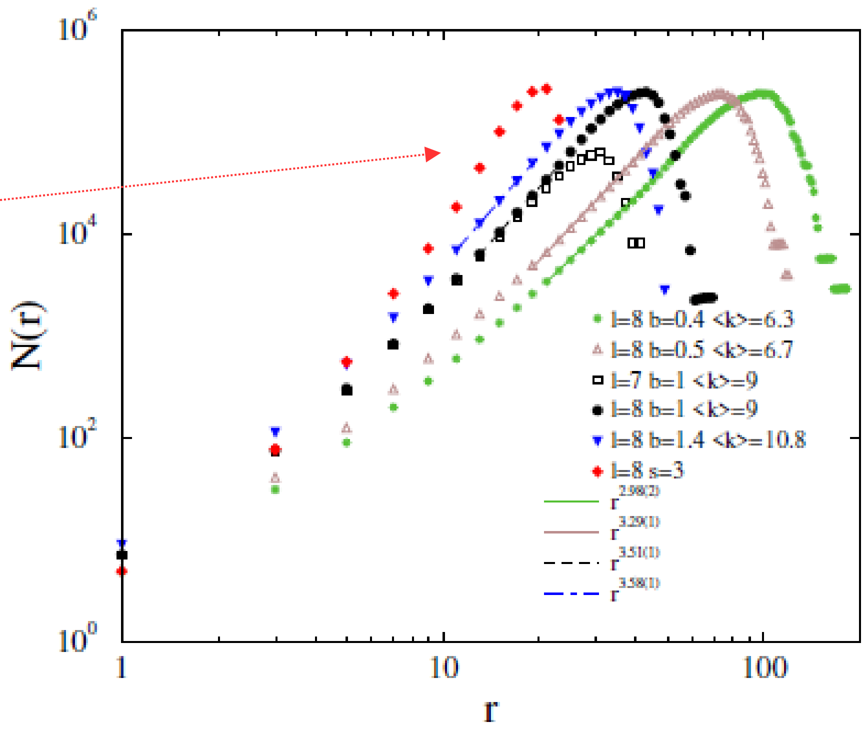

	# Topological features

Topological dimension : $N(r) \sim r^{\,d}$

Breadth-first search algorithm:

$s < 4$: $d \rightarrow \infty$ network

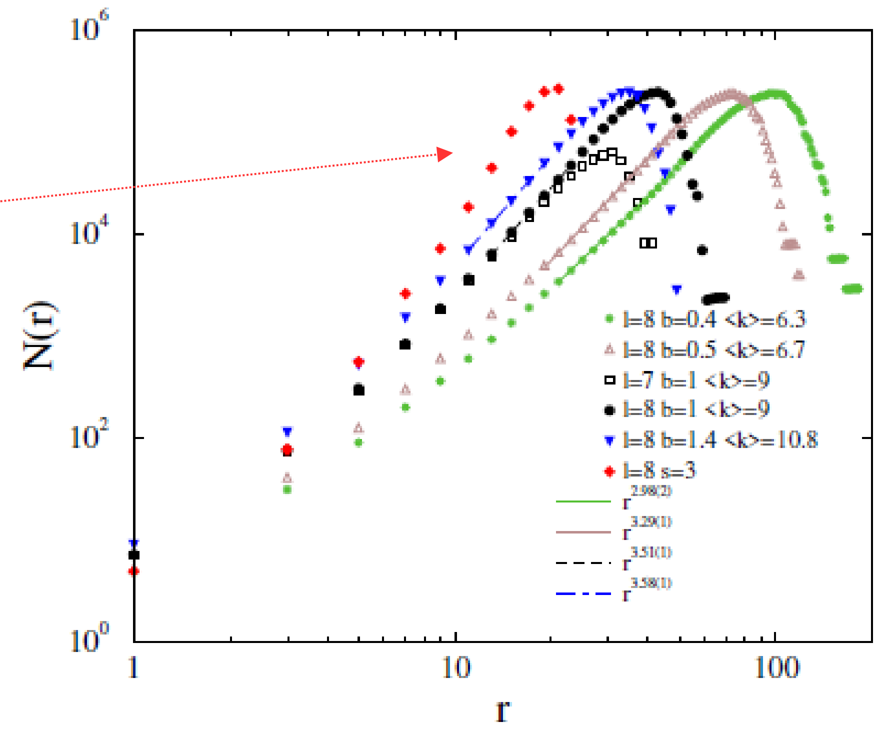

Topological features

Topological dimension : $N(r) \sim r^{d}$

Breadth-first search algorithm:

$s < 4$: $d \rightarrow \infty$ network

$s = 4$: $\langle k \rangle$ dependent, continuously changing d

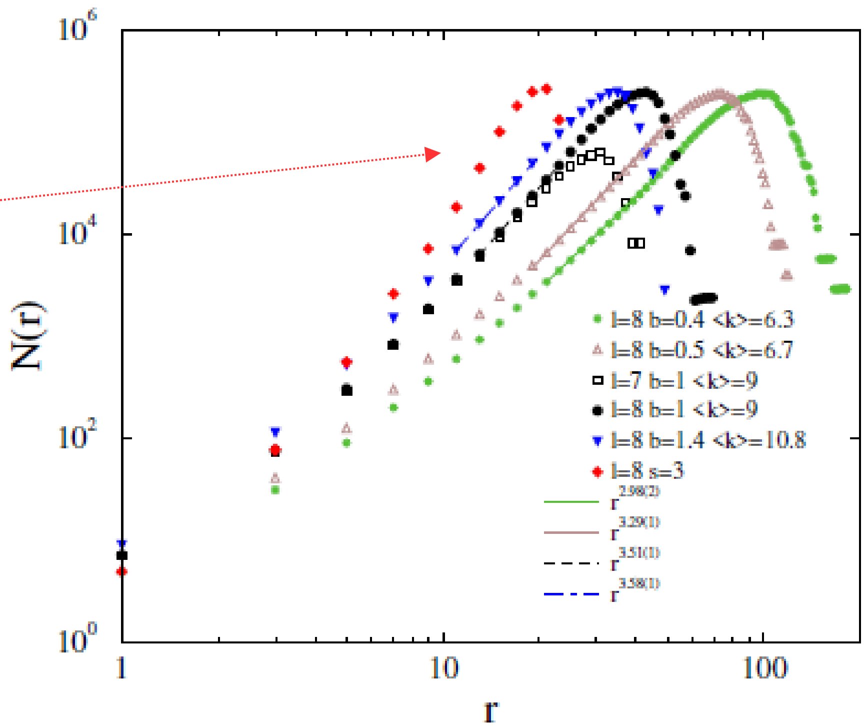

Topological features

Topological dimension : $N(r) \sim r^{\,d}$

Breadth-first search algorithm:

$s < 4$: $d \rightarrow \infty$ network

$s = 4$: $\langle k \rangle$ dependent, continuously changing d

$s > 4$ $d \rightarrow 0$

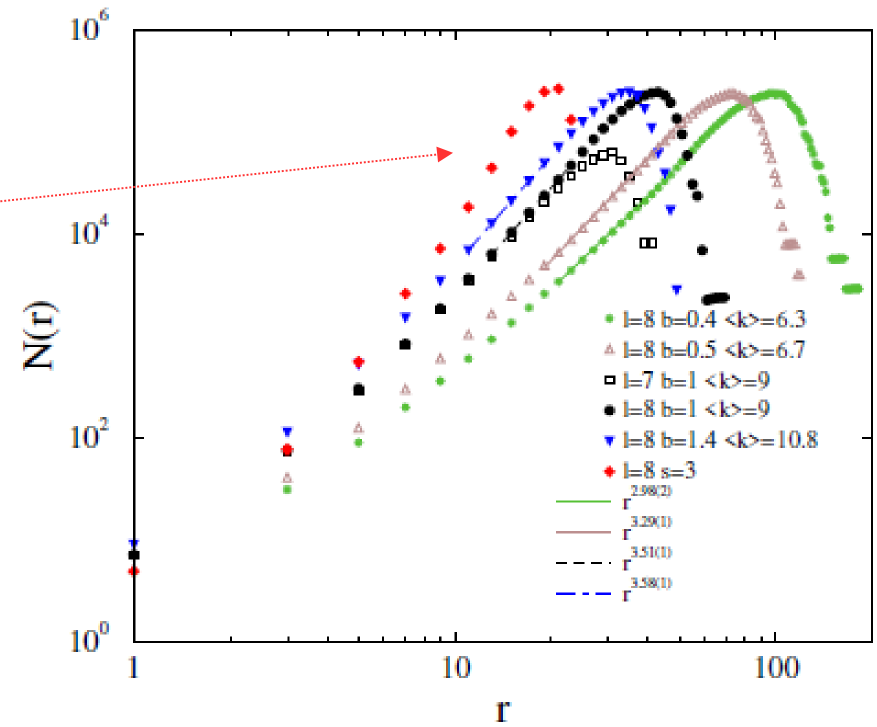

Topological features

Topological dimension : $N(r) \sim r^{\,d}$

Breadth-first search algorithm:

$s < 4$: $d \to \infty$ network

<u>$s = 4$: $\langle k \rangle$ dependent, continuously changing d</u>

$s > 4$ $d \to 0$

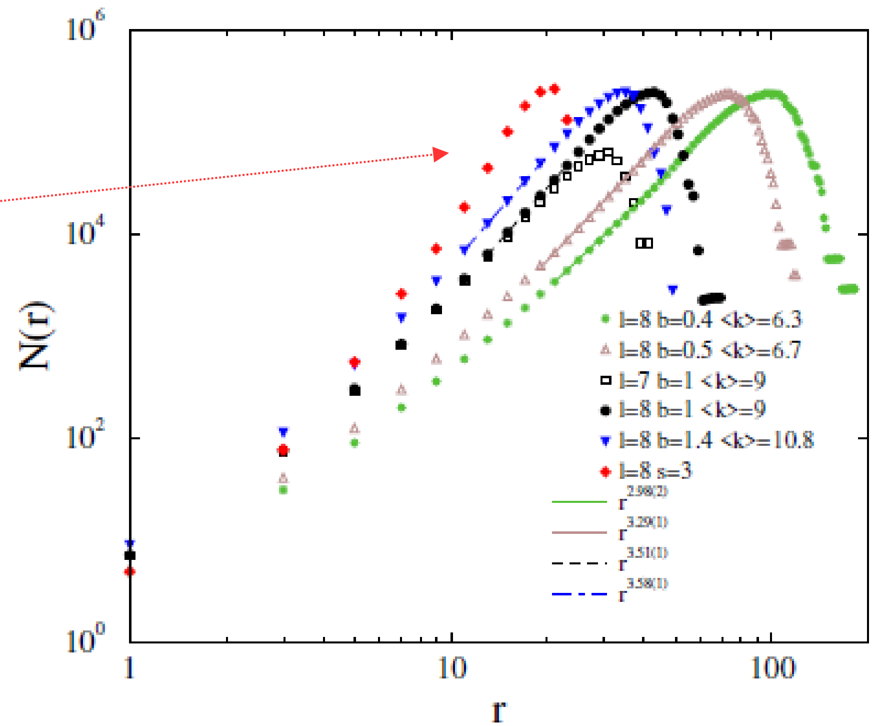

Due to the embedding $R \sim 2^{\,l} \to p(R) \sim R^{\,-s}$

Topological features

Topological dimension : $N(r) \sim r^{\,d}$

Breadth-first search algorithm:

$s < 4$: $d \rightarrow \infty$ network

$s = 4$: <*k*> dependent, continuously changing *d*

$s > 4$ $d \rightarrow 0$

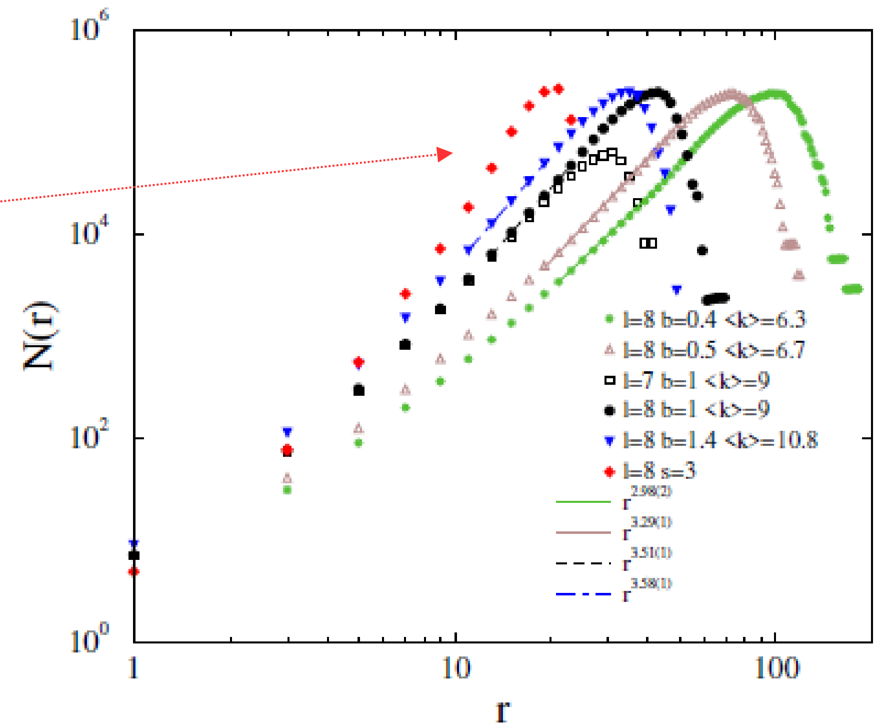

Due to the embedding $R \sim 2^{\,l} \rightarrow$ $p(R) \sim R^{\,-s}$

Clustering coeff. $$C = \frac{1}{N}\sum_i 2n_i/k_i(k_i-1)$$

Topological features

Topological dimension : $N(r) \sim r^{\,d}$

Breadth-first search algorithm:

$s < 4$: $d \to \infty$ network

<u>$s = 4$: <k> dependent, continuously changing d</u>

$s > 4$ $d \to 0$

Due to the embedding $R \sim 2^{\,l} \to p(R) \sim R^{\,-s}$

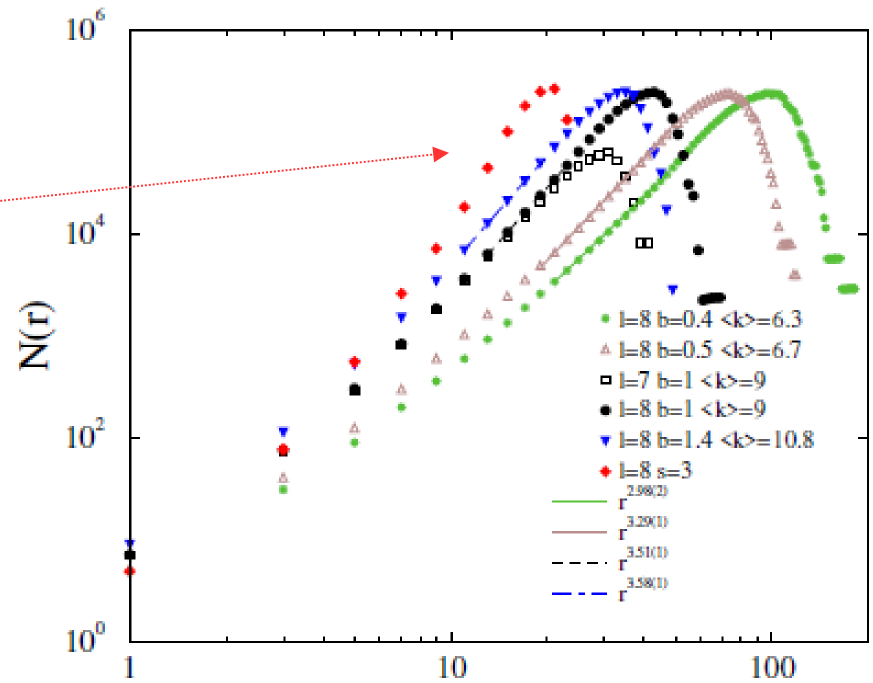

Clustering coeff. $$C = \frac{1}{N}\sum_i 2n_i/k_i(k_i-1)$$ $$C_r = \langle k \rangle / N.$$

Topological features

Topological dimension : $N(r) \sim r^{d}$

Breadth-first search algorithm:

$s < 4$: $d \to \infty$ network

<u>$s = 4$: $<k>$ dependent, continuously changing d</u>

$s > 4$ $d \to 0$

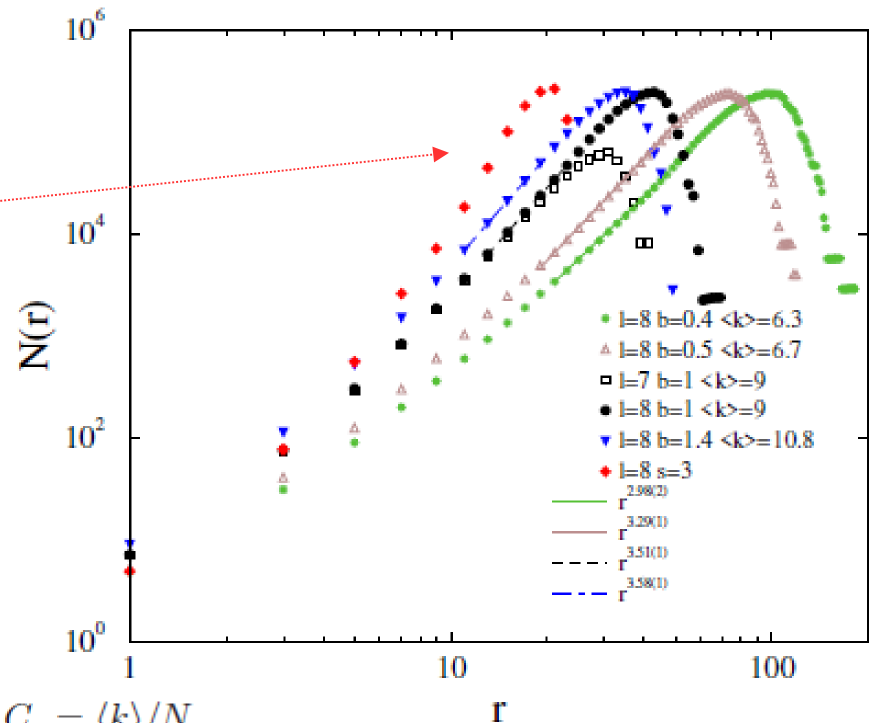

Due to the embedding $R \sim 2^{l} \to p(R) \sim R^{-s}$

Clustering coeff. $$C = \frac{1}{N}\sum_i 2n_i/k_i(k_i-1)$$ $$C_r = \langle k \rangle / N.$$

Average pathlength $$\mathcal{L} = \frac{1}{N(N-1)}\sum_{j\neq i} d(i,j)$$

Topological features

Topological dimension : $N(r) \sim r^{d}$

Breadth-first search algorithm:

$s < 4$: $d \rightarrow \infty$ network

<u>$s = 4$: $<k>$ dependent, continuously changing d</u>

$s > 4$ $d \rightarrow 0$

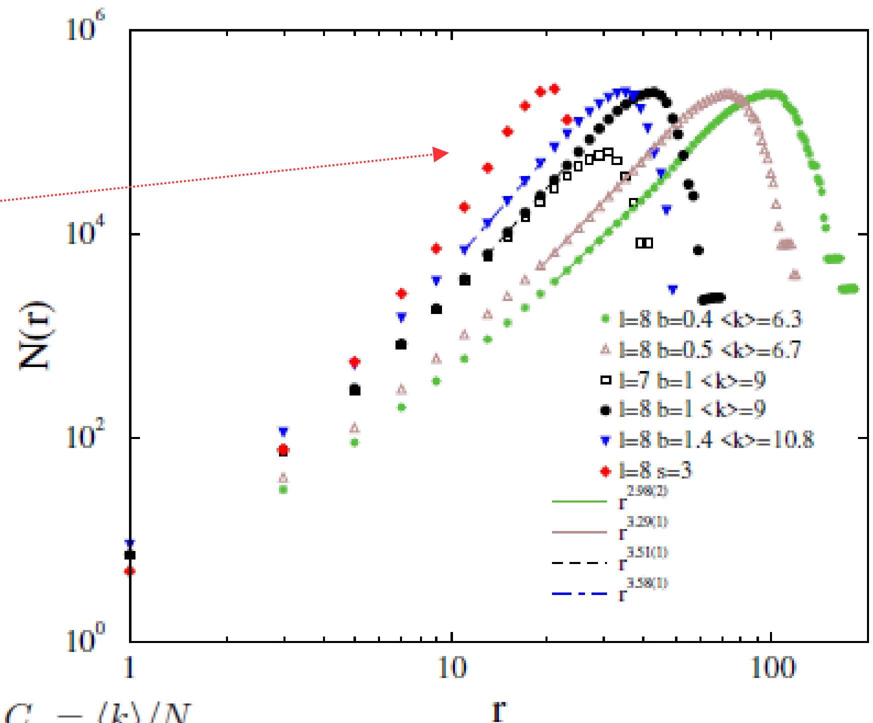

Due to the embedding $R \sim 2^{l} \rightarrow p(R) \sim R^{-s}$

Clustering coeff. $$C = \frac{1}{N}\sum_i 2n_i/k_i(k_i-1)$$ $$C_r = \langle k \rangle / N.$$

Average pathlength $$\mathcal{L} = \frac{1}{N(N-1)}\sum_{j\neq i} d(i,j)$$ $$\mathcal{L}_r = \frac{\ln(N) - 0.5772}{\ln\langle k \rangle} + 1/2$$

Topological features

Topological dimension : $N(r) \sim r^{d}$

Breadth-first search algorithm:

$s < 4$: $d \rightarrow \infty$ network

<u>$s = 4$: $<k>$ dependent, continuously changing d</u>

$s > 4$ $d \rightarrow 0$

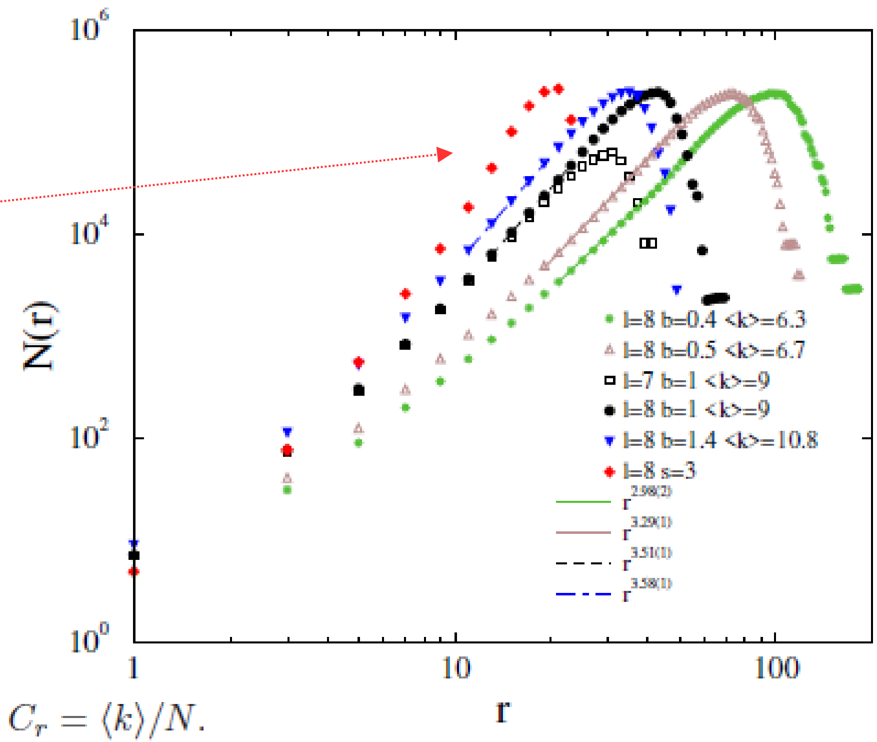

Due to the embedding $R \sim 2^{l} \rightarrow p(R) \sim R^{-s}$

Clustering coeff.
$$C = \frac{1}{N} \sum_i 2n_i/k_i(k_i - 1)$$
$$C_r = \langle k \rangle / N.$$

Average pathlength
$$\mathcal{L} = \frac{1}{N(N-1)} \sum_{j \neq i} d(i,j)$$
$$\mathcal{L}_r = \frac{\ln(N) - 0.5772}{\ln\langle k \rangle} + 1/2$$

Small world coeff
$$\sigma = \frac{C/C_r}{\mathcal{L}/\mathcal{L}_r}$$

Topological features

Topological dimension : $N(r) \sim r^{d}$

Breadth-first search algorithm:

$s < 4$: $d \to \infty$ network

$s = 4$: <k> dependent, continuously changing d

$s > 4$ $d \to 0$

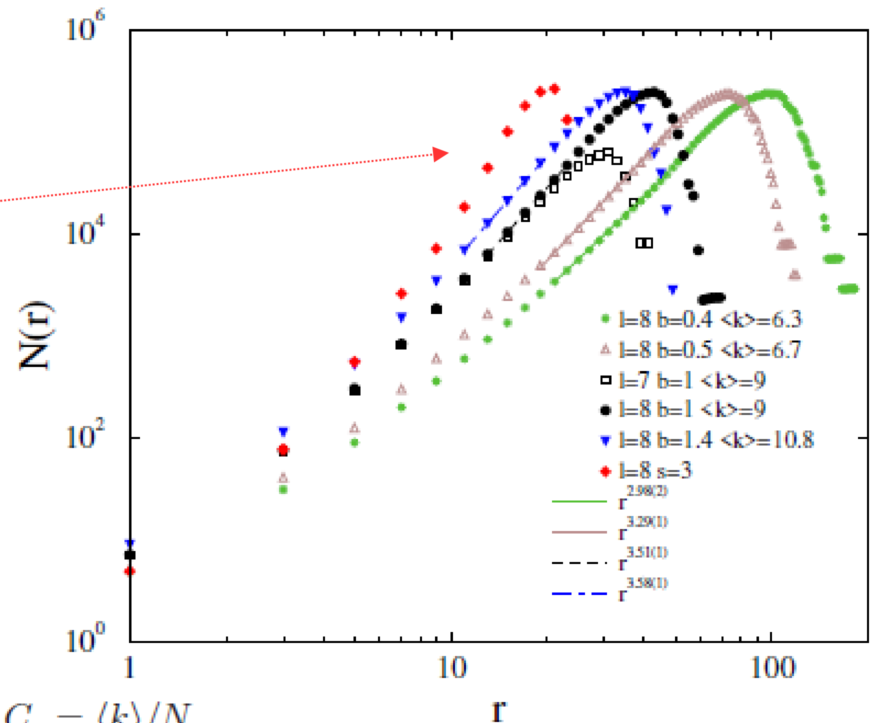

Due to the embedding $R \sim 2^{l} \to p(R) \sim R^{-s}$

Clustering coeff. $$C = \frac{1}{N}\sum_i 2n_i/k_i(k_i-1) \qquad C_r = \langle k\rangle/N.$$

Average pathlength $$\mathcal{L} = \frac{1}{N(N-1)}\sum_{j\neq i} d(i,j) \qquad \mathcal{L}_r = \frac{\ln(N) - 0.5772}{\ln\langle k\rangle} + 1/2$$

Small world coeff $$\sigma = \frac{C/C_r}{\mathcal{L}/\mathcal{L}_r}$$

σ ~ 47 >> 1 : Small world network (finite dimensional)

Simulation SIR SCA model

Simulation SIR SCA model

Synchronous (SCA), discrete time updates: $t = 1,2,3, \ldots. T$

Simulation SIR SCA model

Synchronous (SCA), discrete time updates: $t = 1,2,3, \ldots. T$

Seed initialization: susceptible: $x(j) = 0$ for $j \in (0,N)$

Simulation SIR SCA model

Synchronous (SCA), discrete time updates: $t = 1,2,3, \ldots. T$

Seed initialization: susceptible: $x(j) = 0$ for $j \in (0,N)$

infected : $x(i) = 1$ with i: random site(s)

Simulation SIR SCA model

Synchronous (SCA), discrete time updates: $t = 1,2,3, \ldots. T$

Seed initialization: susceptible: $x(j) = 0$ for $j \in (0,N)$

infected : $x(i) = 1$ with i: random site(s)

Infection : $x'(j) = 1$ if $x(j) = 0$ and $\exists\ x(j_{neigh}) = 1$ with probability: λ

Simulation SIR SCA model

Synchronous (SCA), discrete time updates: $t = 1,2,3, \dots T$

Seed initialization: susceptible: $x(j) = 0$ for $j \in (0,N)$

infected : $x(i) = 1$ with i: random site(s)

Infection : $x'(j) = 1$ if $x(j) = 0$ and $\exists\ x(j_{neigh}) = 1$ with probability: λ

Recovery (or death): $x'(j) = -1$ if $x(j) = 1$ with probability: $\nu = (1-\lambda)$

Simulation SIR SCA model

Synchronous (SCA), discrete time updates: $t = 1,2,3, \ldots. T$

Seed initialization: susceptible: $x(j) = 0$ for $j \in (0,N)$

infected : $x(i) = 1$ with i: random site(s)

Infection : $x'(j) = 1$ if $x(j) = 0$ and $\exists\ x(j_{neigh}) = 1$ with probability: λ

Recovery (or death): $x'(j) = -1$ if $x(j) = 1$ with probability: $\nu = (1-\lambda)$

Diffusion: $x'(j) = x(j_{neigh})$, $x'(j_{neigh}) = x(j)$, if previous conditions failed

Simulation SIR SCA model

Synchronous (SCA), discrete time updates: $t = 1,2,3, \ldots. T$

Seed initialization: susceptible: $x(j) = 0$ for $j \in (0,N)$

infected : $x(i) = 1$ with i: random site(s)

Infection : $x'(j) = 1$ if $x(j) = 0$ and $\exists\ x(j_{neigh}) = 1$ with probability: λ

Recovery (or death): $x'(j) = -1$ if $x(j) = 1$ with probability: $\nu = (1-\lambda)$

Diffusion: $x'(j) = x(j_{neigh})$, $x'(j_{neigh}) = x(j)$, if previous conditions failed

Alternating (back-forth) sweeping to avoid bias

Simulation SIR SCA model

Synchronous (SCA), discrete time updates: $t = 1,2,3, \ldots. T$

Seed initialization: susceptible: $x(j) = 0$ for $j \in (0,N)$

infected : $x(i) = 1$ with i: random site(s)

Infection : $x'(j) = 1$ if $x(j) = 0$ and $\exists\ x(j_{neigh}) = 1$ with probability: λ

Recovery (or death): $x'(j) = -1$ if $x(j) = 1$ with probability: $\nu = (1-\lambda)$

Diffusion: $x'(j) = x(j_{neigh})$, $x'(j_{neigh}) = x(j)$, if previous conditions failed

Alternating (back-forth) sweeping to avoid bias

2d, ***3d*** lattices, *L=4000, 2000, 1000,* ***160, 100*** periodic boundary cond.

Simulation SIR SCA model

Synchronous (SCA), discrete time updates: $t = 1,2,3, \ldots. T$

Seed initialization: susceptible: $x(j) = 0$ for $j \in (0,N)$

infected : $x(i) = 1$ with i: random site(s)

Infection : $x'(j) = 1$ if $x(j) = 0$ and $\exists\ x(j_{neigh}) = 1$ with probability: λ

Recovery (or death): $x'(j) = -1$ if $x(j) = 1$ with probability: $\nu = (1-\lambda)$

Diffusion: $x'(j) = x(j_{neigh})$, $x'(j_{neigh}) = x(j)$, if previous conditions failed

Alternating (back-forth) sweeping to avoid bias

2d, ***3d*** lattices, $L=4000, 2000, 1000,$ ***160, 100*** periodic boundary cond.

HMN-s with: $l_{max} = 6,7,8$ -> $N=16384, 65536, 262144$

Simulation SIR SCA model

Synchronous (SCA), discrete time updates: $t = 1,2,3, \ldots. T$

Seed initialization: susceptible: $x(j) = 0$ for $j \in (0,N)$

infected : $x(i) = 1$ with i: random site(s)

Infection : $x'(j) = 1$ if $x(j) = 0$ and $\exists\ x(j_{neigh}) = 1$ with probability: λ

Recovery (or death): $x'(j) = -1$ if $x(j) = 1$ with probability: $\nu = (1-\lambda)$

Diffusion: $x'(j) = x(j_{neigh})$, $x'(j_{neigh}) = x(j)$, if previous conditions failed

Alternating (back-forth) sweeping to avoid bias

2d, ***3d*** lattices, $L=4000, 2000, 1000,$ ***160, 100*** periodic boundary cond.

HMN-s with: $l_{max} = 6,7,8$ -> $N=16384, 65536, 262144$

Density of infected sites : $I_r(t) = 1/N \sum_{i=1}^{N} \delta(x_i, 1)$

Simulation SIR SCA model

Synchronous (SCA), discrete time updates: $t = 1,2,3, \ldots. T$

Seed initialization: susceptible: $x(j) = 0$ for $j \in (0,N)$

infected : $x(i) = 1$ with i: random site(s)

Infection : $x'(j) = 1$ if $x(j) = 0$ and $\exists\ x(j_{neigh}) = 1$ with probability: λ

Recovery (or death): $x'(j) = -1$ if $x(j) = 1$ with probability: $\nu = (1-\lambda)$

Diffusion: $x'(j) = x(j_{neigh})$, $x'(j_{neigh}) = x(j)$, if previous conditions failed

Alternating (back-forth) sweeping to avoid bias

2d, ***3d*** lattices, *L=4000, 2000, 1000*, ***160, 100*** periodic boundary cond.

HMN-s with: $l_{max} = 6,7,8$ -> N=*16384, 65536, 262144*

Density of infected sites : $I_r(t) = 1/N \sum_{i=1}^{N} \delta(x_i, 1)$

Avalanche size : $S_r = \sum_{i=1}^{N} \sum_{t=1}^{T} \delta(x_i, 1)$

Growth results on homogeneous 2d, 3D lattices

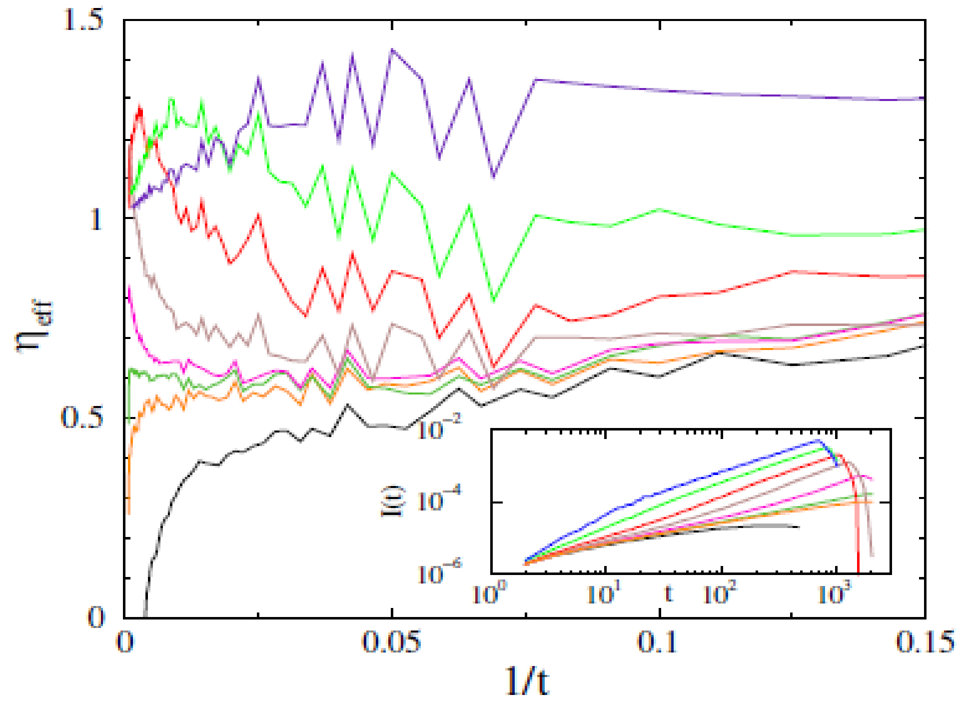

FIG. 3: Effective exponents $\eta_{\rm eff}(t)$ in 2d for $\lambda = 0.4$, 0.406, 0.407, 0.408, 0.41, 0.42, 0.44, 0.5 (bottom to top curves). Inset: initial time evolution of $I(t)$, averaged over runs from 10^4 randomly selected initial random sites. The two distict fixed point behavior can be seen at $\lambda_c = 0.4059(1)$, with $\eta = 0.59(1)$ and the supercitical phase, characterzed by $\eta = 1$.

Growth results on homogeneous 2d, 3D lattices

Local slopes:

$$\eta_{\text{eff}}(t) = \frac{\ln I(t) - \ln I(t')}{\ln(t) - \ln(t')} \ ,$$

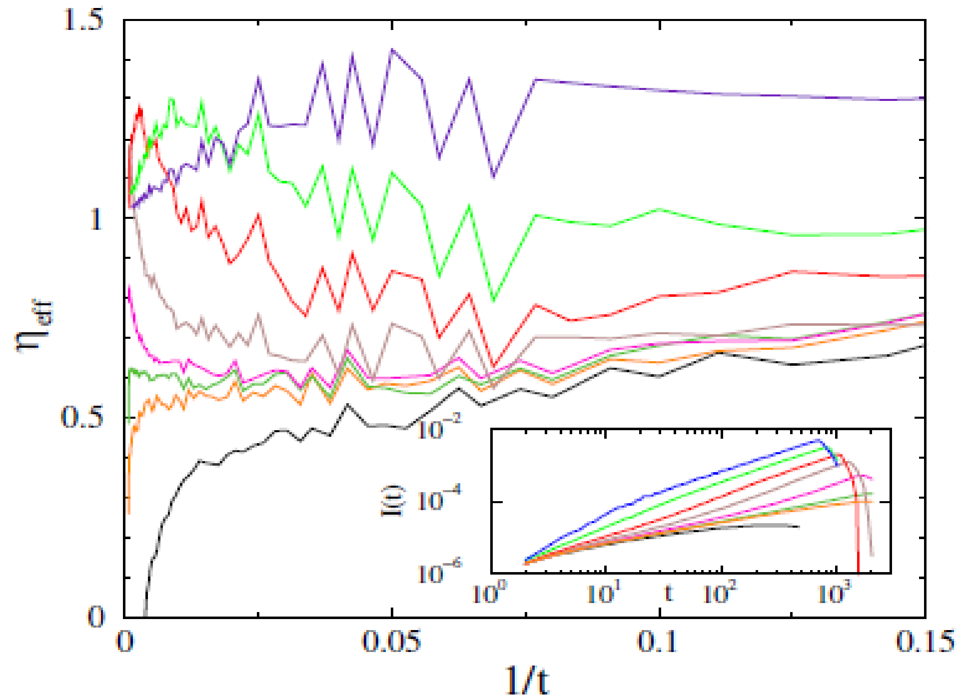

FIG. 3: Effective exponents $\eta_{\text{eff}}(t)$ in 2d for $\lambda = 0.4$, 0.406, 0.407, 0.408, 0.41, 0.42, 0.44, 0.5 (bottom to top curves). Inset: initial time evolution of $I(t)$, averaged over runs from 10^4 randomly selected initial random sites. The two distict fixed point behavior can be seen at $\lambda_c = 0.4059(1)$, with $\eta = 0.59(1)$ and the supercitical phase, characterzed by $\eta = 1$.

Growth results on homogeneous 2d, 3D lattices

Local slopes:

$$\eta_{\rm eff}(t) = \frac{\ln I(t) - \ln I(t')}{\ln(t) - \ln(t')} \ ,$$

In $d = 2$ critical point

at $\lambda_c = 0.4059(1)$

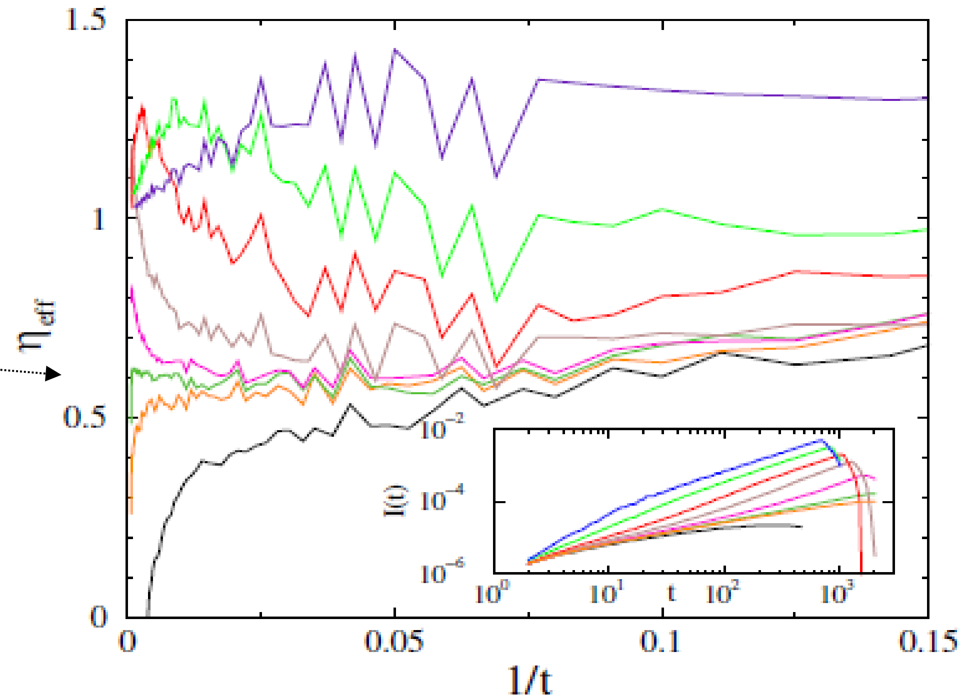

FIG. 3: Effective exponents $\eta_{\rm eff}(t)$ in 2d for $\lambda = 0.4$, 0.406, 0.407, 0.408, 0.41, 0.42, 0.44, 0.5 (bottom to top curves). Inset: initial time evolution of $I(t)$, averaged over runs from 10^4 randomly selected initial random sites. The two distict fixed point behavior can be seen at $\lambda_c = 0.4059(1)$, with $\eta = 0.59(1)$ and the supercitical phase, characterzed by $\eta = 1$.

Growth results on homogeneous 2d, 3D lattices

Local slopes:

$$\eta_{\mathrm{eff}}(t) = \frac{\ln I(t) - \ln I(t')}{\ln(t) - \ln(t')} \ ,$$

In $d = 2$ critical point

at $\lambda_c = 0.4059(1)$

Critical $\eta \sim \eta_{DIP} = 0.586$

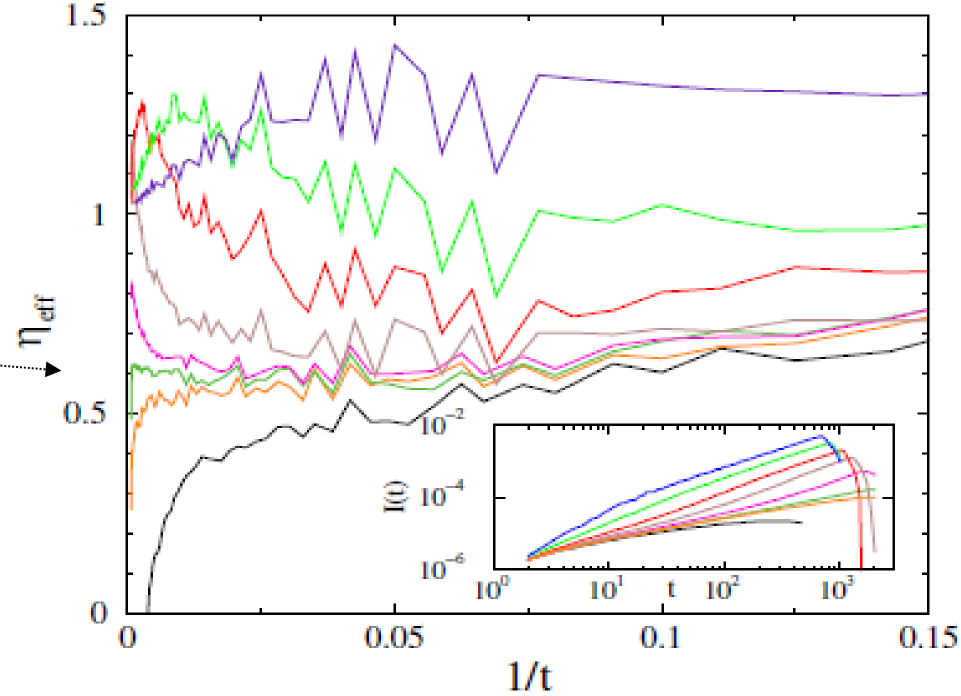

FIG. 3: Effective exponents $\eta_{\mathrm{eff}}(t)$ in 2d for $\lambda = 0.4$, 0.406, 0.407, 0.408, 0.41, 0.42, 0.44, 0.5 (bottom to top curves). Inset: initial time evolution of $I(t)$, averaged over runs from 10^4 randomly selected initial random sites. The two distict fixed point behavior can be seen at $\lambda_c = 0.4059(1)$, with $\eta = 0.59(1)$ and the supercitical phase, characterzed by $\eta = 1$.

Growth results on homogeneous 2d, 3D lattices

Local slopes:

$$\eta_{\rm eff}(t) = \frac{\ln I(t) - \ln I(t')}{\ln(t) - \ln(t')} \ ,$$

In $d = 2$ critical point

at $\lambda_c = 0.4059(1)$

Critical $\eta \sim \eta_{DIP} = 0.586$

Above λ_c $\eta \rightarrow 1$

with overshooting

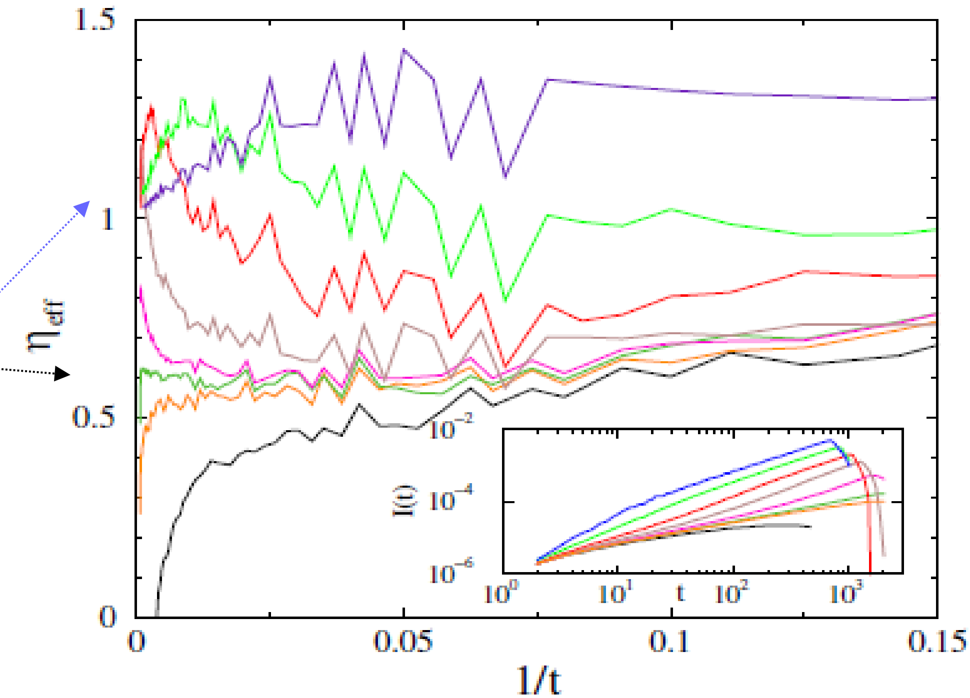

FIG. 3: Effective exponents $\eta_{\rm eff}(t)$ in 2d for $\lambda = 0.4$, 0.406, 0.407, 0.408, 0.41, 0.42, 0.44, 0.5 (bottom to top curves). Inset: initial time evolution of $I(t)$, averaged over runs from 10^4 randomly selected initial random sites. The two distict fixed point behavior can be seen at $\lambda_c = 0.4059(1)$, with $\eta = 0.59(1)$ and the supercitical phase, characterzed by $\eta = 1$.

Growth results on homogeneous 2d, 3D lattices

Local slopes:

$$\eta_{\mathrm{eff}}(t) = \frac{\ln I(t) - \ln I(t')}{\ln(t) - \ln(t')} ,$$

In $d = 2$ critical point

at $\lambda_c = 0.4059(1)$

Critical $\eta \sim \eta_{DIP} = 0.586$

Above λ_c $\eta \rightarrow 1$

with overshooting

When $\xi \to L$: exponential

decay : “Herd immunity”

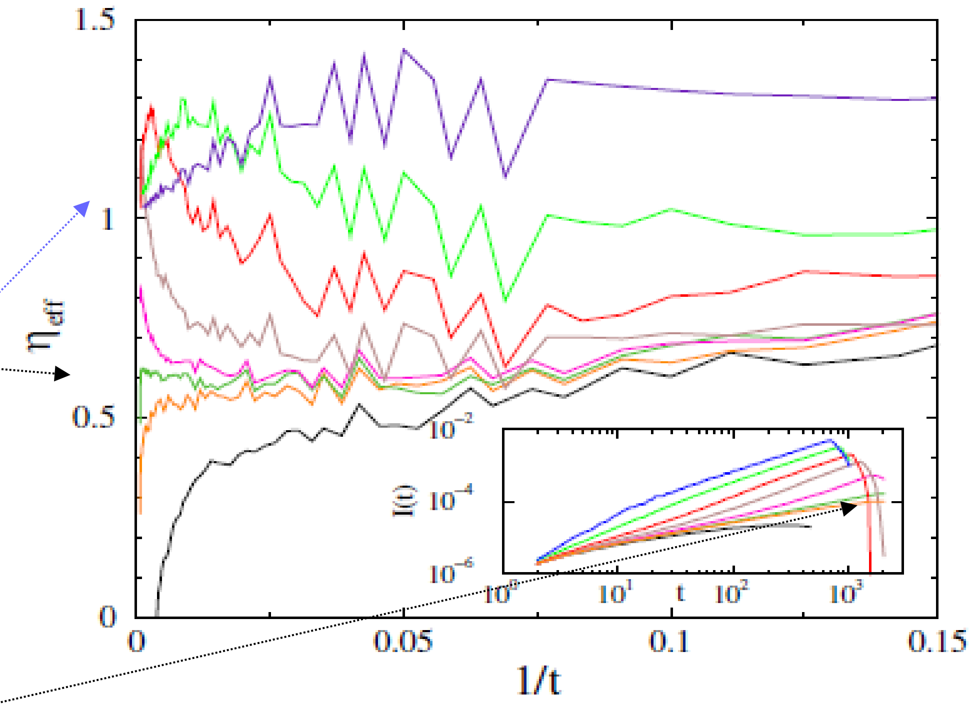

FIG. 3: Effective exponents $\eta_{\mathrm{eff}}(t)$ in 2d for $\lambda = 0.4$, 0.406, 0.407, 0.408, 0.41, 0.42, 0.44, 0.5 (bottom to top curves). Inset: initial time evolution of $I(t)$, averaged over runs from 10^4 randomly selected initial random sites. The two distict fixed point behavior can be seen at $\lambda_c = 0.4059(1)$, with $\eta = 0.59(1)$ and the supercitical phase, characterzed by $\eta = 1$.

Growth results on homogeneous 2d, 3D lattices

Local slopes:

$$\eta_{\text{eff}}(t) = \frac{\ln I(t) - \ln I(t')}{\ln(t) - \ln(t')} \; ,$$

In $d = 2$ critical point

at $\lambda_c = 0.4059(1)$

Critical $\eta \sim \eta_{DIP} = 0.586$

Above λ_c $\eta \rightarrow 1$

with overshooting

When $\xi \rightarrow L$: exponential

decay : “Herd immunity”

In 3d similar situation

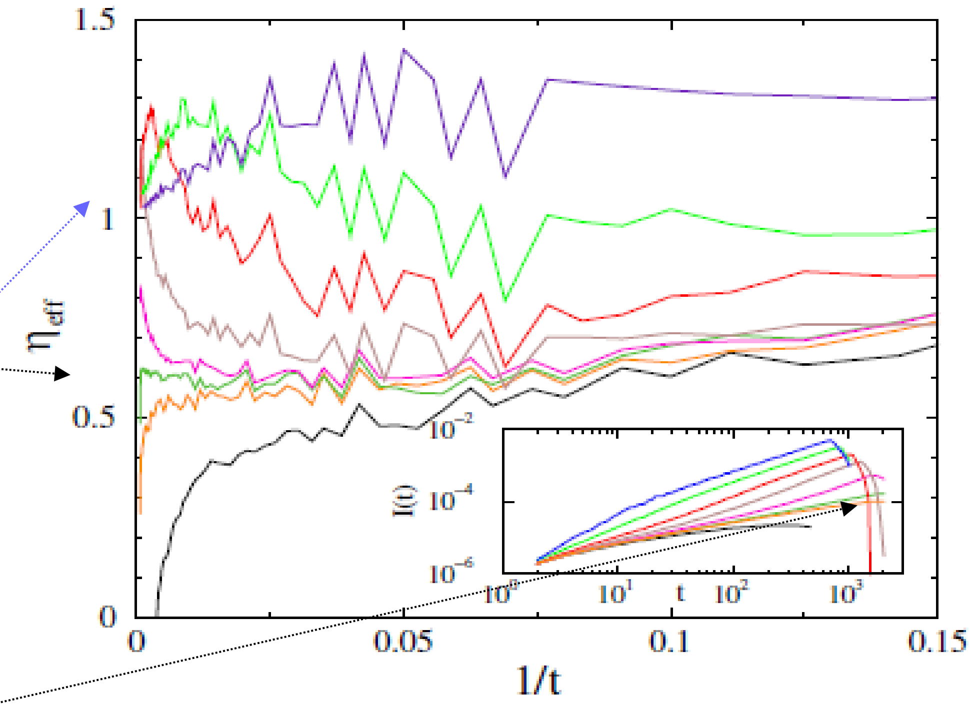

FIG. 3: Effective exponents $\eta_{\text{eff}}(t)$ in 2d for $\lambda = 0.4$, 0.406, 0.407, 0.408, 0.41, 0.42, 0.44, 0.5 (bottom to top curves). Inset: initial time evolution of $I(t)$, averaged over runs from 10^4 randomly selected initial random sites. The two distict fixed point behavior can be seen at $\lambda_c = 0.4059(1)$, with $\eta = 0.59(1)$ and the supercitical phase, characterzed by $\eta = 1$.

Growth results for various HMN-s

$$\lambda = \nu = 1$$

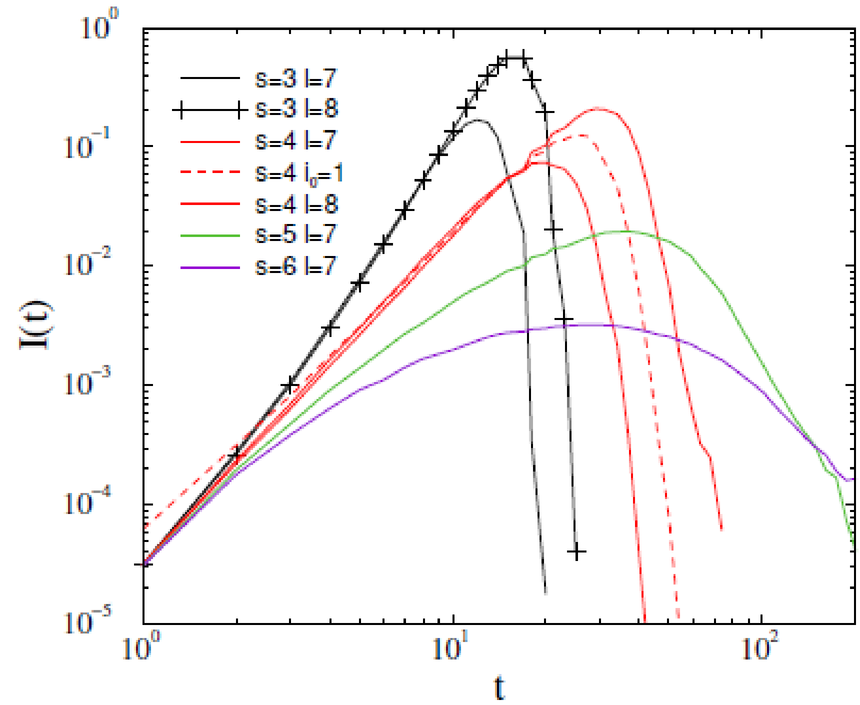

FIG. 4: Density of infected sites in different graphs for $i_0 = 2$, by varying s and the size with $b = 1$ and $\lambda = \nu = 1$ fixed. Thin lines $l_{max} = 7$, thick lines $l_{max} = 8$ data, multiplied by a factor of 4. Only the $s = 4$ curves exhibit PL initially and exponential decay is observable following finite size cutoff, corresponding to heard immunity. The dashed line corresponds to the single seed case: $i_0 = 1$, multiplied by a factor 2.

Growth results for various HMN-s

$$\lambda = \nu = 1$$

Power-laws (PL) at *s=4* (finite dim.)

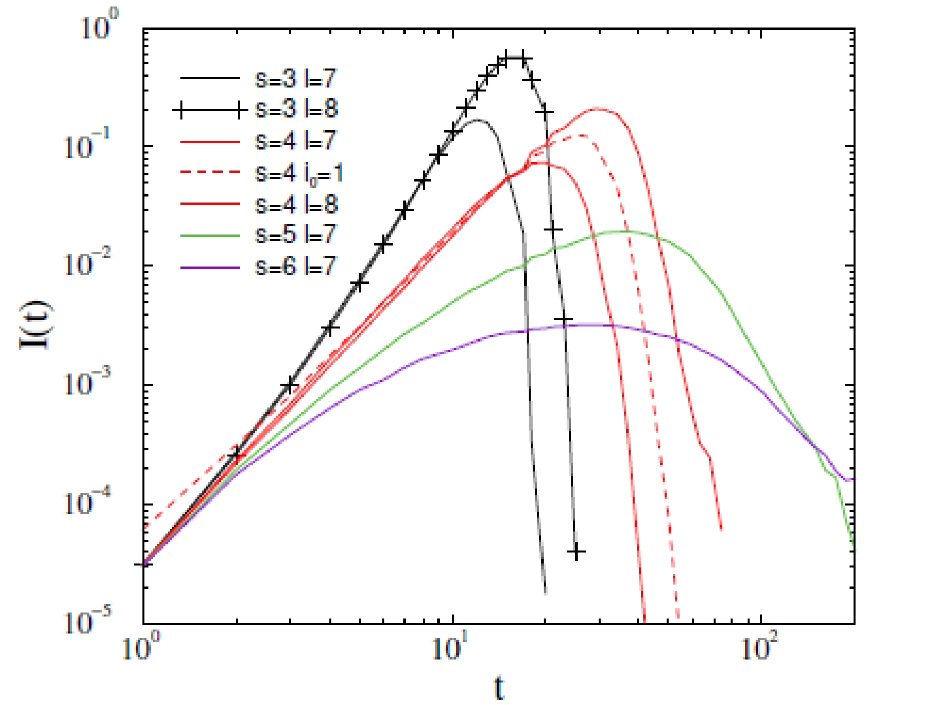

FIG. 4: Density of infected sites in different graphs for $i_0 = 2$, by varying s and the size with $b = 1$ and $\lambda = \nu = 1$ fixed. Thin lines $l_{max} = 7$, thick lines $l_{max} = 8$ data, multiplied by a factor of 4. Only the $s = 4$ curves exhibit PL initially and exponential decay is observable following finite size cutoff, corresponding to heard immunity. The dashed line corresponds to the single seed case: $i_0 = 1$, multiplied by a factor 2.

Growth results for various HMN-s

$$\lambda = \nu = 1$$

Power-laws (PL) at *s=4* (finite dim.)

For *s* < *3* faster than PL

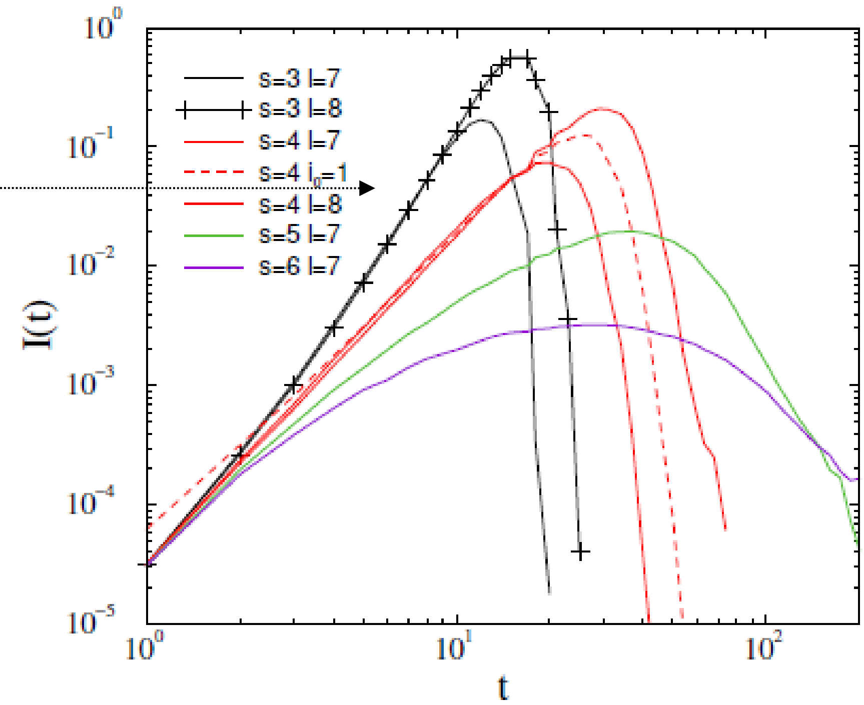

FIG. 4: Density of infected sites in different graphs for $i_0 = 2$, by varying s and the size with $b = 1$ and $\lambda = \nu = 1$ fixed. Thin lines $l_{max} = 7$, thick lines $l_{max} = 8$ data, multiplied by a factor of 4. Only the $s = 4$ curves exhibit PL initially and exponential decay is observable following finite size cutoff, corresponding to heard immunity. The dashed line corresponds to the single seed case: $i_0 = 1$, multiplied by a factor 2.

Growth results for various HMN-s

$$\lambda = \nu = 1$$

Power-laws (PL) at *s=4* (finite dim.)

For *s* < *3* faster than PL

For *s* > *4* slower than PL

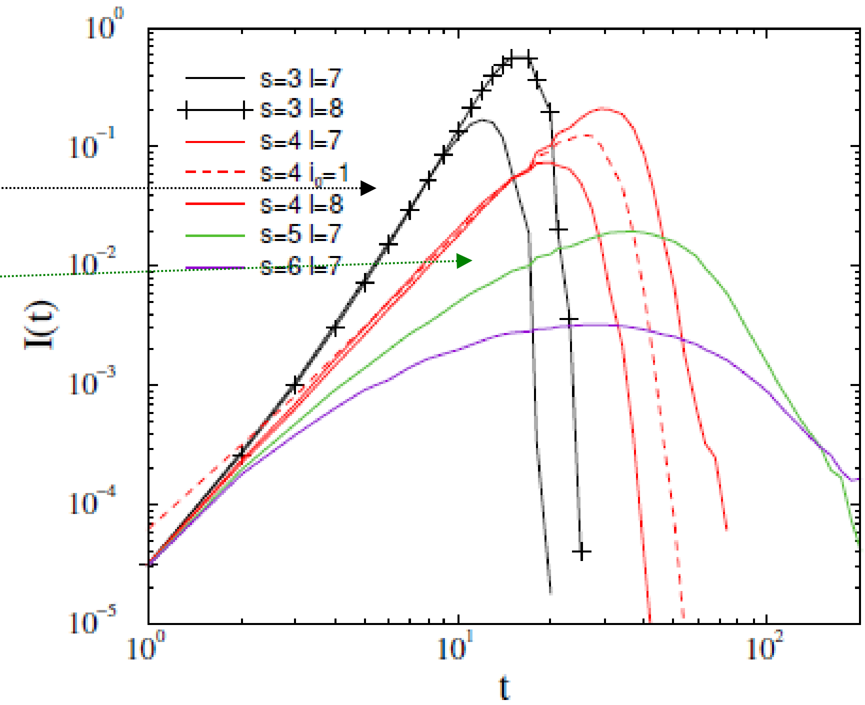

FIG. 4: Density of infected sites in different graphs for $i_0 = 2$, by varying s and the size with $b = 1$ and $\lambda = \nu = 1$ fixed. Thin lines $l_{max} = 7$, thick lines $l_{max} = 8$ data, multiplied by a factor of 4. Only the $s = 4$ curves exhibit PL initially and exponential decay is observable following finite size cutoff, corresponding to heard immunity. The dashed line corresponds to the single seed case: $i_0 = 1$, multiplied by a factor 2.

Growth results for various HMN-s

$$\lambda = \nu = 1$$

Power-laws (PL) at *s=4* (finite dim.)

For *s* < *3* faster than PL

For *s* > *4* slower than PL

Epidemic scales up with the number of seeds (i_0) but PL slope invariance

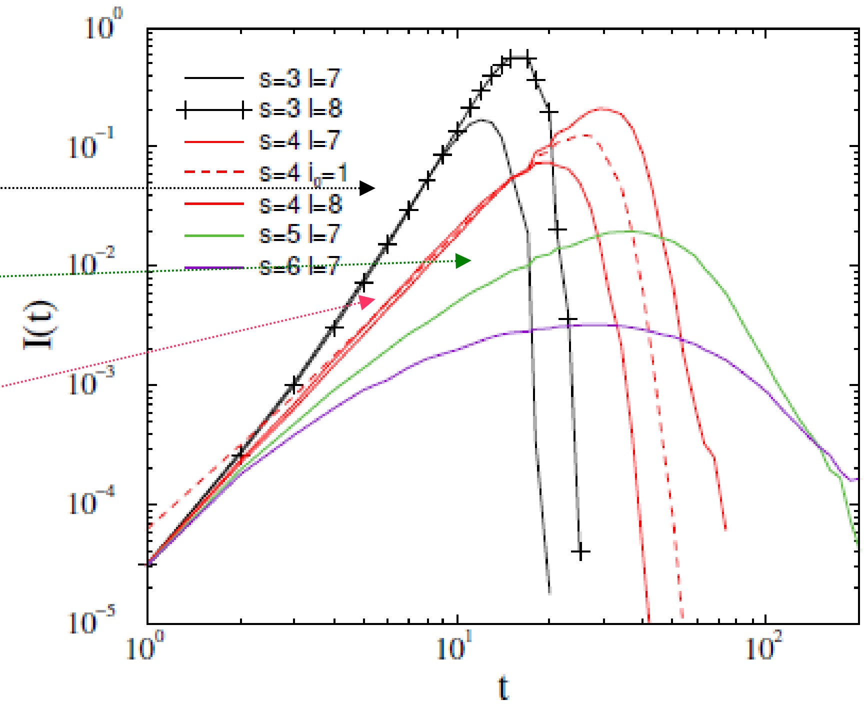

FIG. 4: Density of infected sites in different graphs for $i_0 = 2$, by varying s and the size with $b = 1$ and $\lambda = \nu = 1$ fixed. Thin lines $l_{max} = 7$, thick lines $l_{max} = 8$ data, multiplied by a factor of 4. Only the $s = 4$ curves exhibit PL initially and exponential decay is observable following finite size cutoff, corresponding to heard immunity. The dashed line corresponds to the single seed case: $i_0 = 1$, multiplied by a factor 2.

Results for *s* = *4* HMN

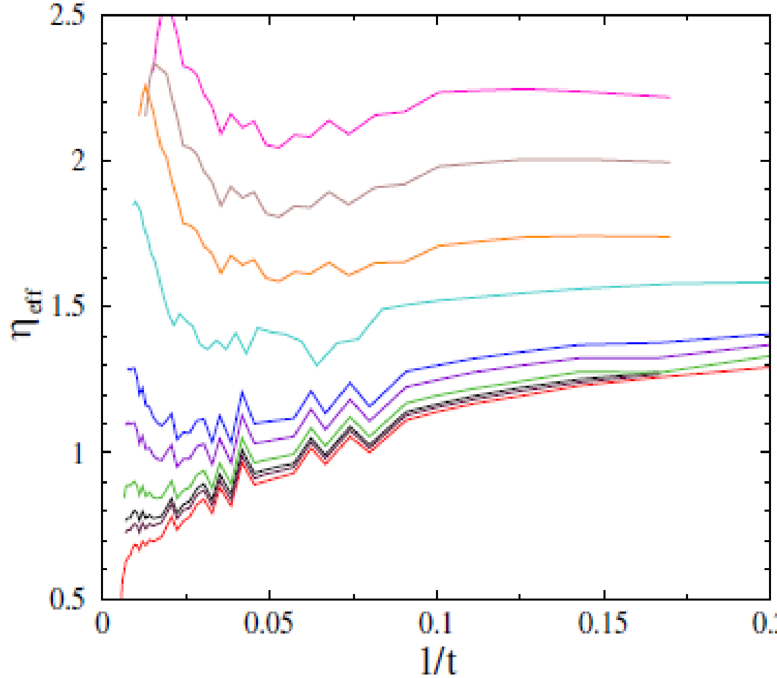

FIG. 6: Effective exponents $\eta_{\rm eff}$ as in Fig. 5, for $s = 4$ and $b = 0.4$ for λ= 0.47, 0.473, 0.475, 0.48, 0.49, 0.5, 0.55, 0.6, 0.7, 0.8 (bottom to top curves). The two distinct fixed point behavior can be seen at $\lambda_c = 0.480(5)$, with $\eta = 0.8(1)$ and the supercritical phase, characterized by $\eta \simeq 2$.

Results for *s = 4* HMN

For $s=4$, $b=0.4$: $d \cong 3$, $\langle k \rangle = 6.3$

Close to the *3d* Euclidean lattice

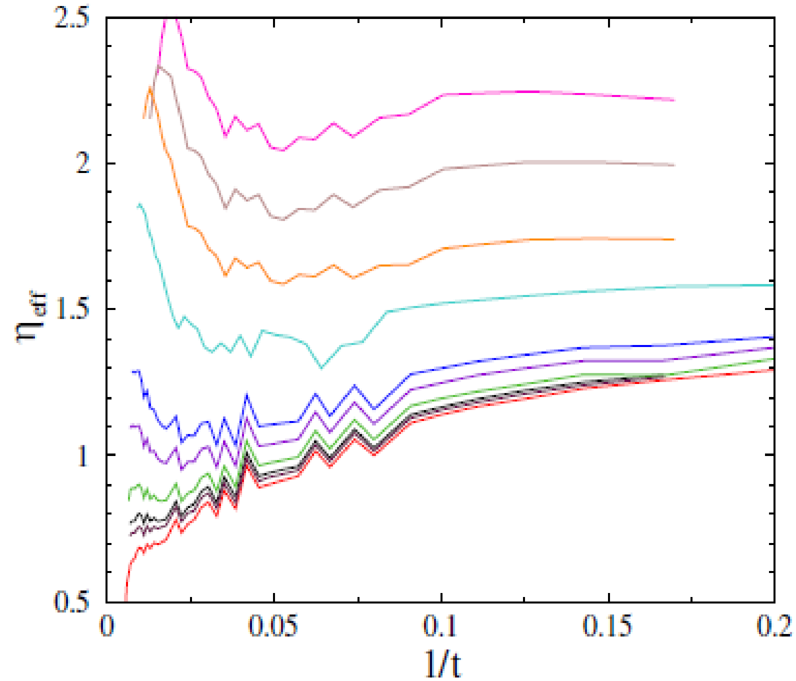

FIG. 6: Effective exponents $\eta_{\rm eff}$ as in Fig. 5, for $s = 4$ and $b = 0.4$ for λ= 0.47, 0.473, 0.475, 0.48, 0.49, 0.5, 0.55, 0.6, 0.7, 0.8 (bottom to top curves). The two distinct fixed point behavior can be seen at $\lambda_c = 0.480(5)$, with $\eta = 0.8(1)$ and the supercritical phase, characterized by $\eta \simeq 2$.

Results for *s = 4* HMN

For $s=4$, $b=0.4$: $d \cong 3$, $<k>=6.3$

Close to the *3d* Euclidean lattice

Still at λ_c : $\eta = 0.8(1) \leftrightarrow \eta_{DIP} = 0.53(2)$

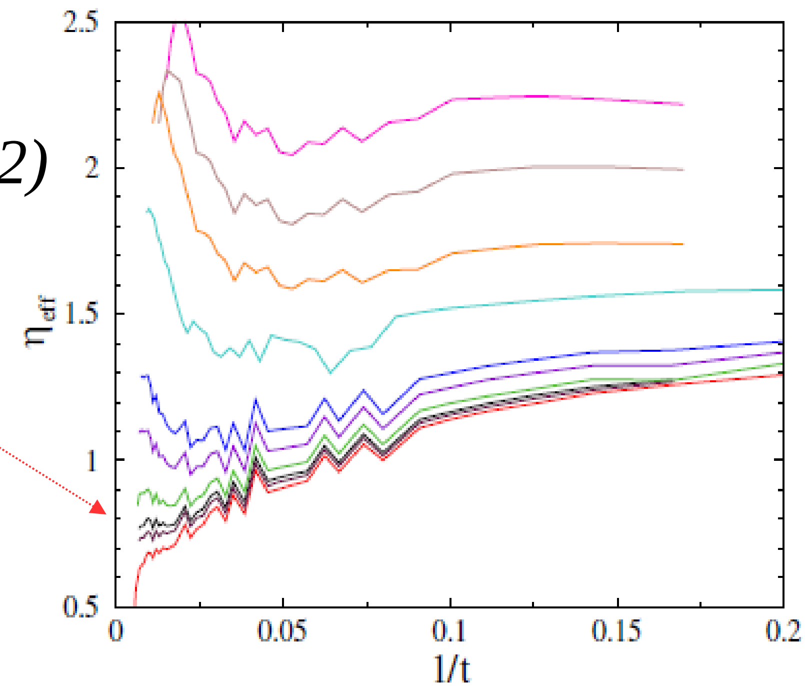

FIG. 6: Effective exponents η_{eff} as in Fig. 5, for $s = 4$ and $b = 0.4$ for λ= 0.47, 0.473, 0.475, 0.48, 0.49, 0.5, 0.55, 0.6, 0.7, 0.8 (bottom to top curves). The two distinct fixed point behavior can be seen at $\lambda_c = 0.480(5)$, with $\eta = 0.8(1)$ and the supercritical phase, characterized by $\eta \simeq 2$.

Results for *s = 4* HMN

For $s=4$, $b=0.4$: $d \cong 3$, $\langle k \rangle=6.3$

Close to the *3d* Euclidean lattice

Still at λ_c : $\eta = 0.8(1) \leftrightarrow \eta_{DIP} = 0.53(2)$

For: $\lambda > \lambda_c = 0.480(5)$:
$\eta \to 2 \approx d - 1$

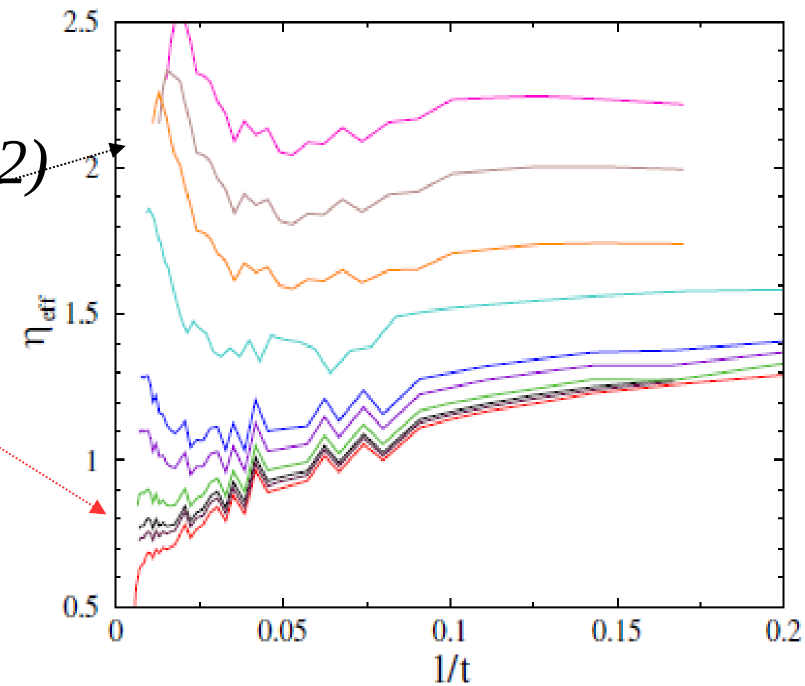

FIG. 6: Effective exponents $\eta_{\rm eff}$ as in Fig. 5, for $s = 4$ and $b = 0.4$ for λ= 0.47, 0.473, 0.475, 0.48, 0.49, 0.5, 0.55, 0.6, 0.7, 0.8 (bottom to top curves). The two distinct fixed point behavior can be seen at $\lambda_c = 0.480(5)$, with $\eta = 0.8(1)$ and the supercritical phase, characterized by $\eta \simeq 2$.

Results for *s = 4* HMN

For $s=4$, $b=0.4$: $d \cong 3$, $\langle k \rangle = 6.3$

Close to the *3d* Euclidean lattice

Still at λ_c : $\eta = 0.8(1) \leftrightarrow \eta_{DIP} = 0.53(2)$

For: $\lambda > \lambda_c = 0.480(5)$:
$\eta \rightarrow 2 \approx d - 1$

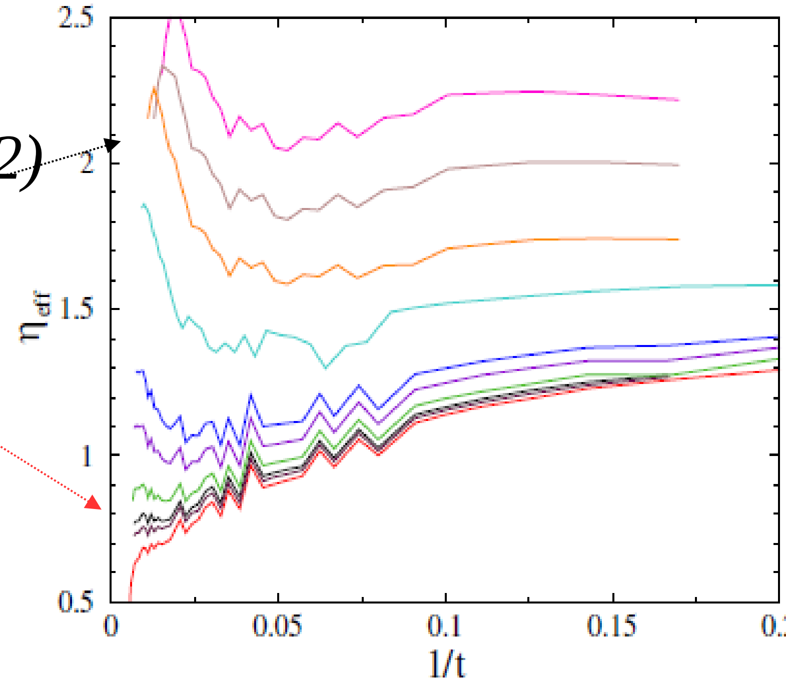

FIG. 6: Effective exponents $\eta_{\rm eff}$ as in Fig. 5, for $s = 4$ and $b = 0.4$ for λ= 0.47, 0.473, 0.475, 0.48, 0.49, 0.5, 0.55, 0.6, 0.7, 0.8 (bottom to top curves). The two distinct fixed point behavior can be seen at $\lambda_c = 0.480(5)$, with $\eta = 0.8(1)$ and the supercritical phase, characterized by $\eta \simeq 2$.

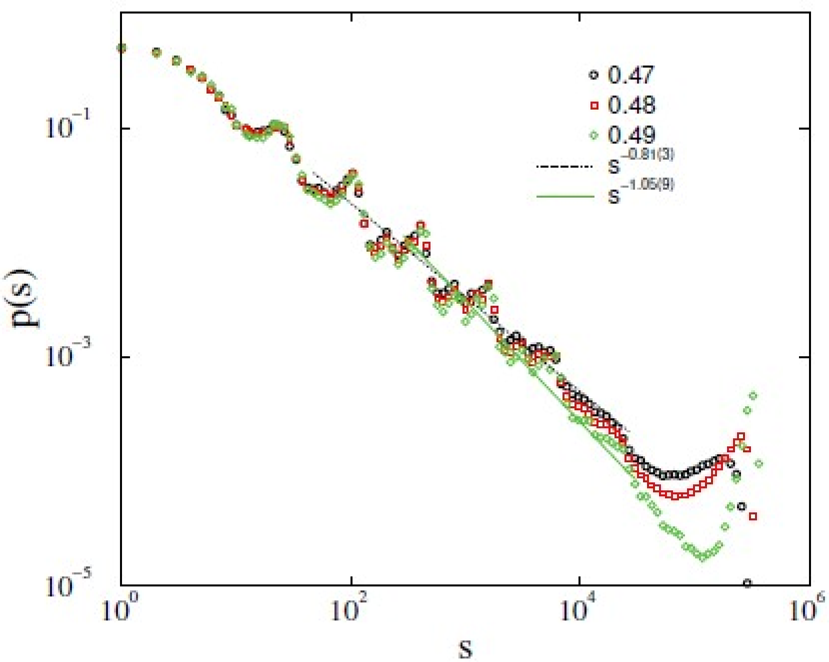

Avalanche size: $\tau = 1.05(5) \leftrightarrow \tau_{DIP} = 1.20(2)$

Results for *s = 4* HMN

For other $<k>$-s continuously varying exponents
Topological heterogeneity changes the scaling behavior !!!

For $s=4$, $b=0.4$: $d \cong 3$, $<k>=6.3$

Close to the *3d* Euclidean lattice

Still at λ_c : $\eta = 0.8(1) \leftrightarrow \eta_{DIP} = 0.53(2)$

For: $\lambda > \lambda_c = 0.480(5)$:
$\eta \to 2 \approx d - 1$

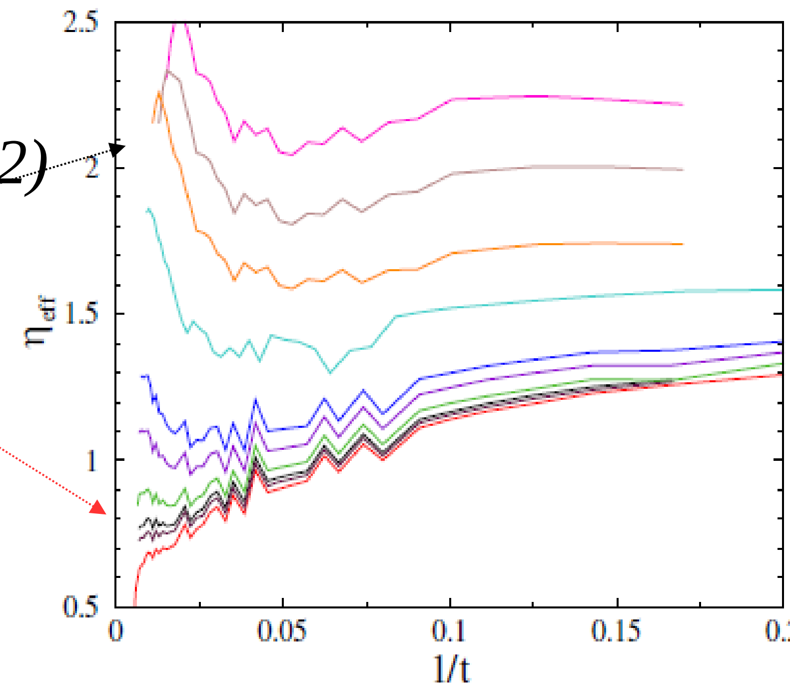

FIG. 6: Effective exponents $\eta_{\rm eff}$ as in Fig. 5, for $s = 4$ and $b = 0.4$ for λ= 0.47, 0.473, 0.475, 0.48, 0.49, 0.5, 0.55, 0.6, 0.7, 0.8 (bottom to top curves). The two distinct fixed point behavior can be seen at $\lambda_c = 0.480(5)$, with $\eta = 0.8(1)$ and the supercritical phase, characterized by $\eta \simeq 2$.

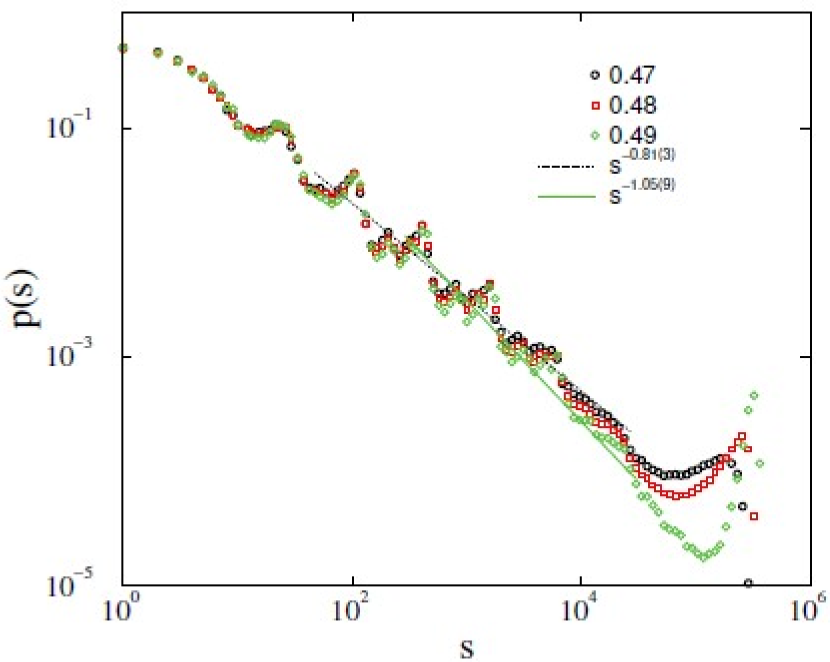

Avalanche size: $\tau = 1.05(5) \leftrightarrow \tau_{DIP} = 1.20(2)$

The effect of diffusion on the SIR model

SIR reactions in a bosonic representation (with soft particle restrictions):

$$I \underset{\kappa}{\overset{\lambda}{\rightleftarrows}} 2I\,, \quad I \xrightarrow{\sigma} \emptyset\,, \quad I \xrightarrow{\mu} R\,, \quad I + R \xrightarrow{\nu} R\,.$$

The non-diffusive SIR process on a lattice: **dynamical isotropic percolation (DIP) class.**

- *Rs diffuse*: **DSIR** $\Rightarrow$ field action ($S \leftrightarrow \emptyset$)

$$\mathcal{A} = \int \mathrm{d}^d x \mathrm{d}t \Big\{ \underbrace{\tilde{\mathcal{I}} \left[\partial_t - D_I \left(\tau - \nabla^2 \right) + \frac{g}{2} \left(2\mathcal{R} - \tilde{\mathcal{I}} \right) \right] \mathcal{I}}_{\text{DIP}} + \tilde{\mathcal{R}} \left(\partial_t - D_R \nabla^2 \right) \mathcal{R} - \tilde{\mathcal{R}} \mathcal{I} \Big\}\,.$$

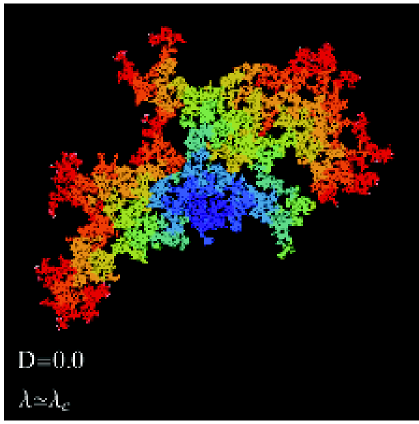

- DIP (SIR)[a] displays **duality symmetry**[b]:

$$\boxed{\tilde{\mathcal{I}}(x,t) \leftrightarrow -\mathcal{R}(x,-t) = -\int_{-\infty}^{-t} dt' \mathcal{I}(x,t')}$$

- Diffusion of R renders violation of the symmetry

$$\partial_t \mathcal{R} = D_R \nabla^2 \mathcal{R} + \mathcal{I} \;\Rightarrow\; \cancel{\tilde{\mathcal{I}}(x,t) \leftrightarrow -\mathcal{R}(x,-t)}$$

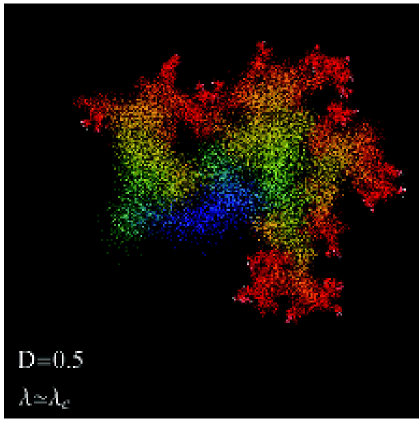

[a] P. Grassberger, Math. Biosci. **63**, 157-172 (1983).
[b] H-K. Janssen *et al*, Ann. Phys. **315**, 147-192 (2005).
[c] Géza Ódor, Phys. Rev. E. **103**, 062112 (2021).

Seed simulation

Exponents (**two species**):

- Initial slip exponent: $N_{I|R} \sim t^{\theta_{I|R}}$;
- Survival probability: $P_{\text{sur}} \sim t^{-\delta}$;
- Mean square spreading: $R^2 \sim t^{Z_{I|R}} = t^{2/z_{I|R}}$.

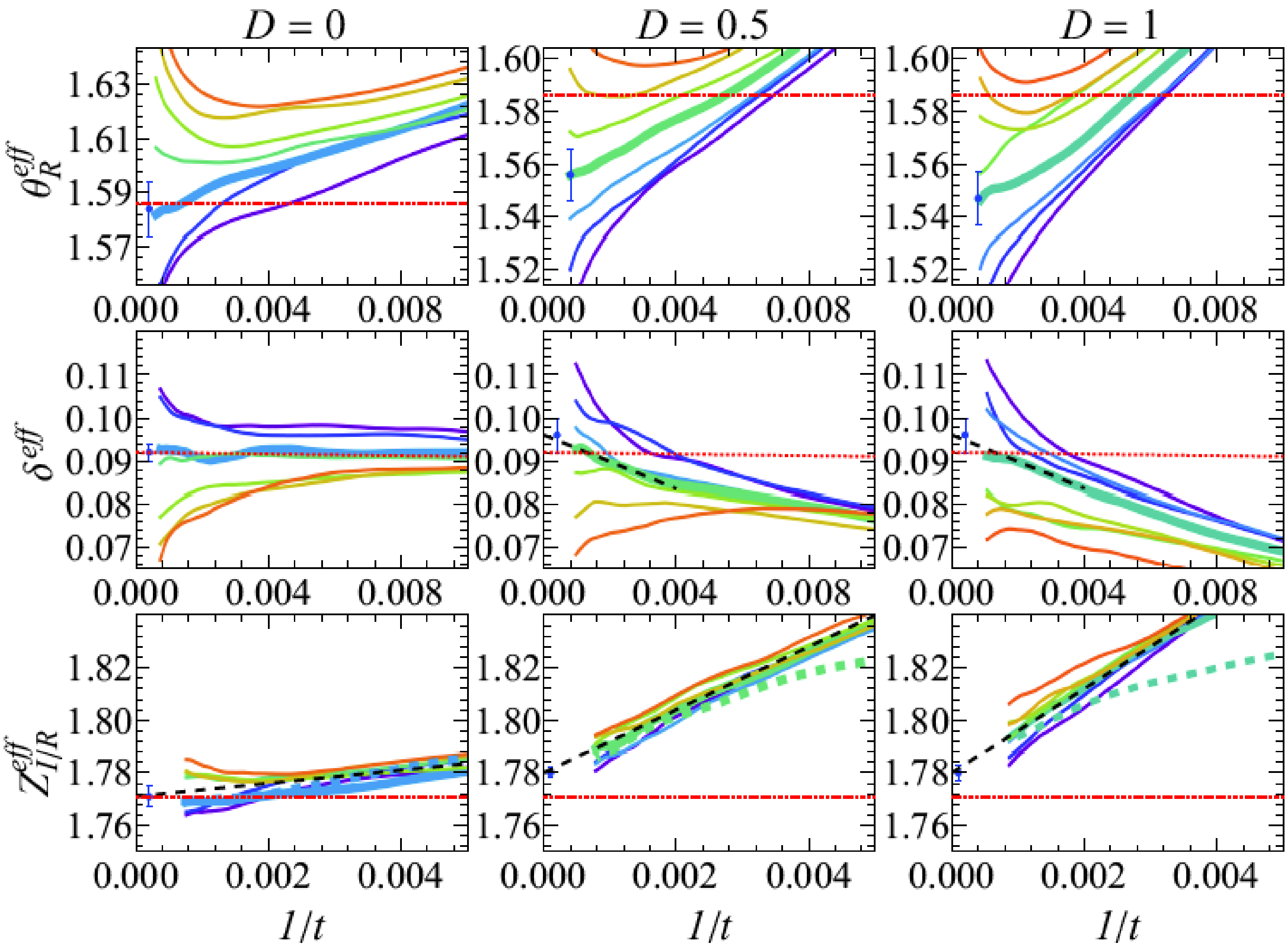

Finite-size scaling analysis for the static case

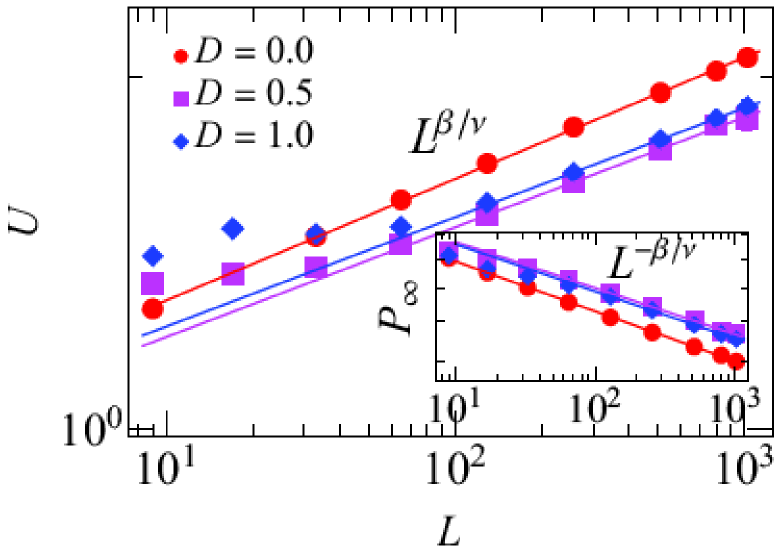

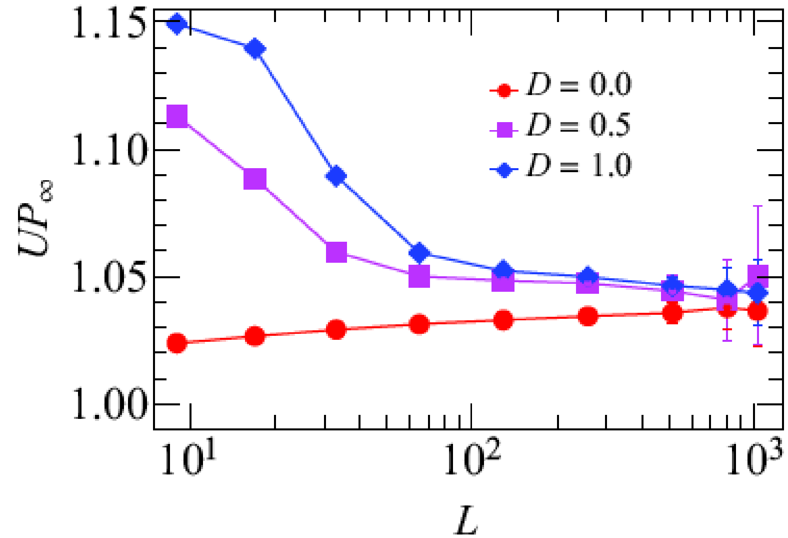

- Freeze the system once the border is hit;
- At criticality [1]: mean cluster size $\langle N_{R\infty}\rangle \sim L^{\gamma/\nu}$, percolation prob. $P_\infty \sim L^{-\beta/\nu}$, $U = \langle N^2_{R\infty}\rangle / \langle N_{R\infty}\rangle^2 \sim L^{\beta/\nu} \Rightarrow UP_\infty \sim$ const.;
- **DSIR: scaling regime is only reached for large L;**
- $\delta = \beta/\nu_\parallel = \beta Z/2\nu$, $(2\beta+\gamma)/\nu d = 1$ ✘

	β/ν	γ/ν	$\nu_\parallel$
DIP Refs.[2]	0.1042	1.792	1.5057
$D = 0$	0.1040(2)	1.810(2)	1.51(1)
$D = 0.5$	0.096(2)	1.764(4)	1.46(1)
$D = 1.0$	0.093(3)	1.755(3)	1.47(1)

[1] D. de Souza *et al.*, JSAT, **2011** (3), P03006 (2011).
[2] https://en.wikipedia.org/wiki/Percolation_critical_exponents

Super-spreader hot-spot in the diffusive HMN case

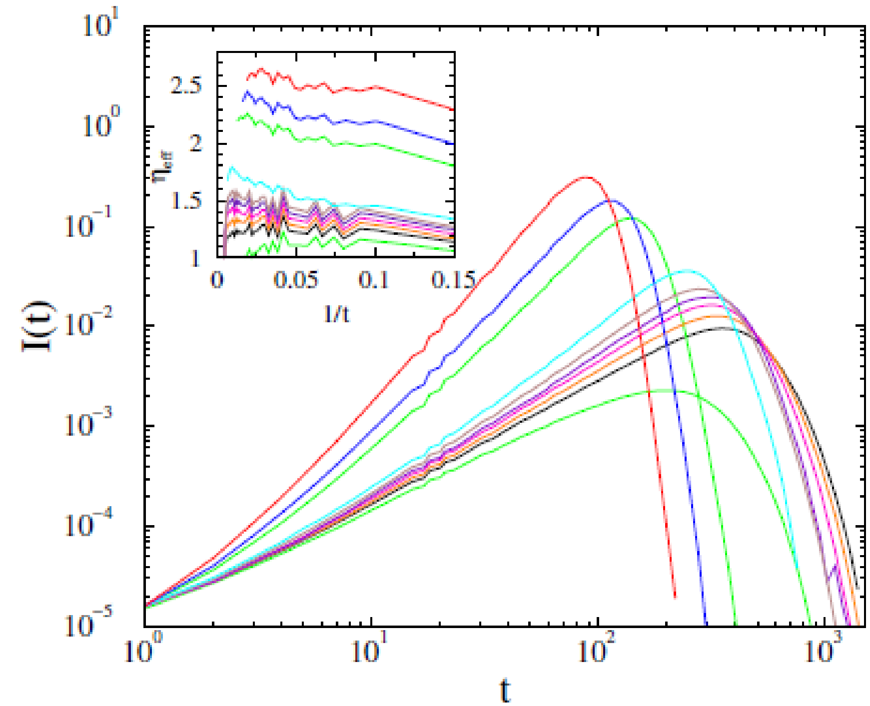

FIG. 11: The effect of a single hot-spot for the diffusive mode in graphs with $s = 4$, $b = 1$ and $\lambda = 0.22$, 0.23, 0.235, 0.24 0.245, 0.25, 0.26, 0.4, 0.5 (bottom to top curves). Inset: Local slopes of the same. The asymptotic critical and supercritical effective exponents are roughly the same as in the non-diffusive homogeneous SIR.

Super-spreader hot-spot in the diffusive HMN case

At single site $\lambda_i = 1$ is set

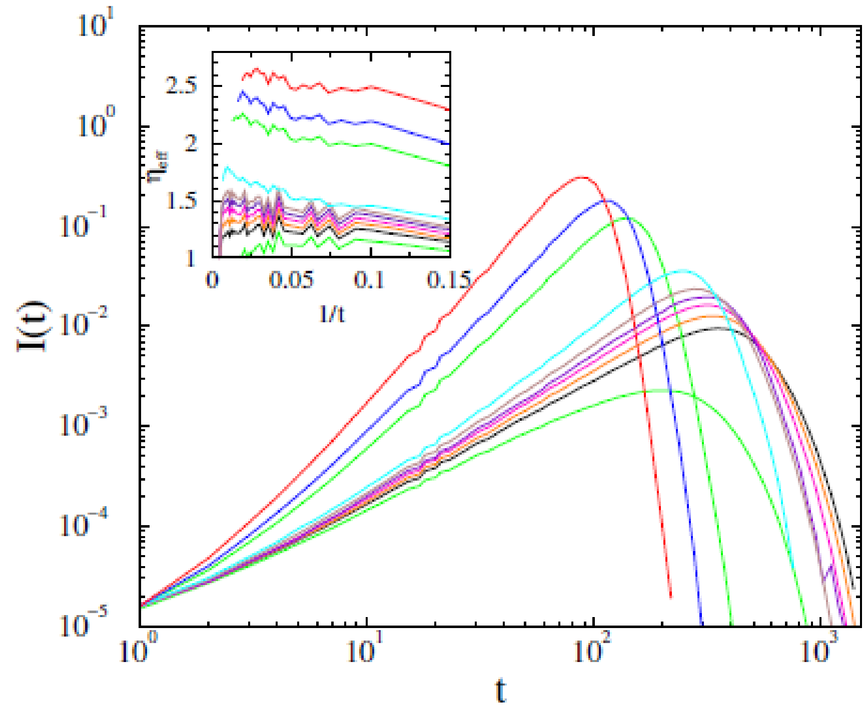

FIG. 11: The effect of a single hot-spot for the diffusive mode in graphs with $s = 4$, $b = 1$ and $\lambda = 0.22, 0.23, 0.235, 0.24$ 0.245, 0.25, 0.26, 0.4, 0.5 (bottom to top curves). Inset: Local slopes of the same. The asymptotic critical and super critical effective exponents are roughly the same as in the non-diffusive homogeneous SIR.

Super-spreader hot-spot in the diffusive HMN case

At single site $\lambda_i = 1$ is set

Scaling exponents do not change

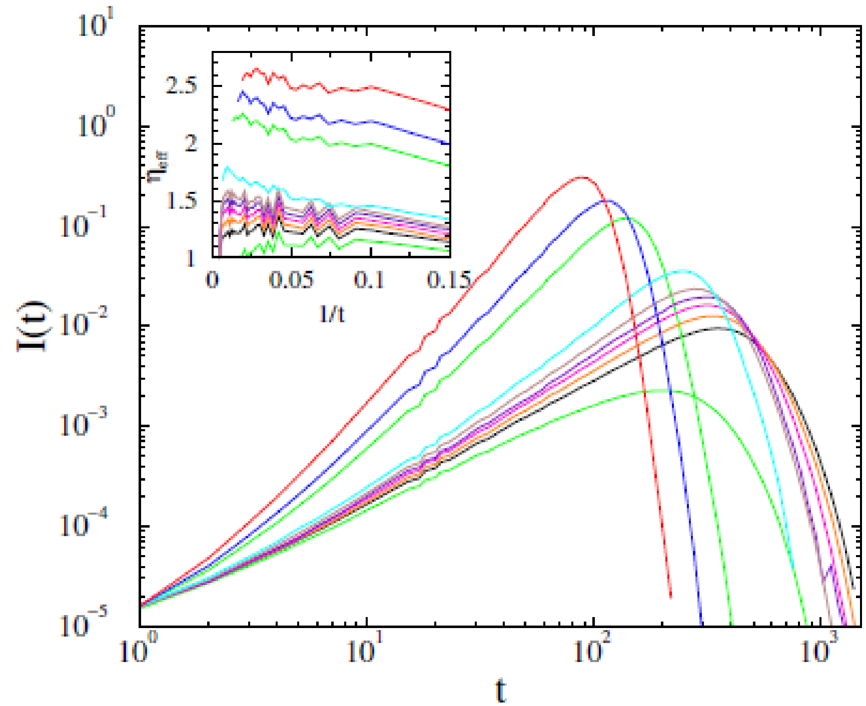

FIG. 11: The effect of a single hot-spot for the diffusive mode in graphs with $s = 4$, $b = 1$ and $\lambda = 0.22, 0.23, 0.235, 0.24$ $0.245, 0.25, 0.26, 0.4, 0.5$ (bottom to top curves). Inset: Local slopes of the same. The asymptotic critical and supercritical effective exponents are roughly the same as in the non-diffusive homogeneous SIR.

Super-spreader hot-spot in the diffusive HMN case

At single site $\lambda_i = 1$ is set

Scaling exponents do not change

Size grows due to diffusion

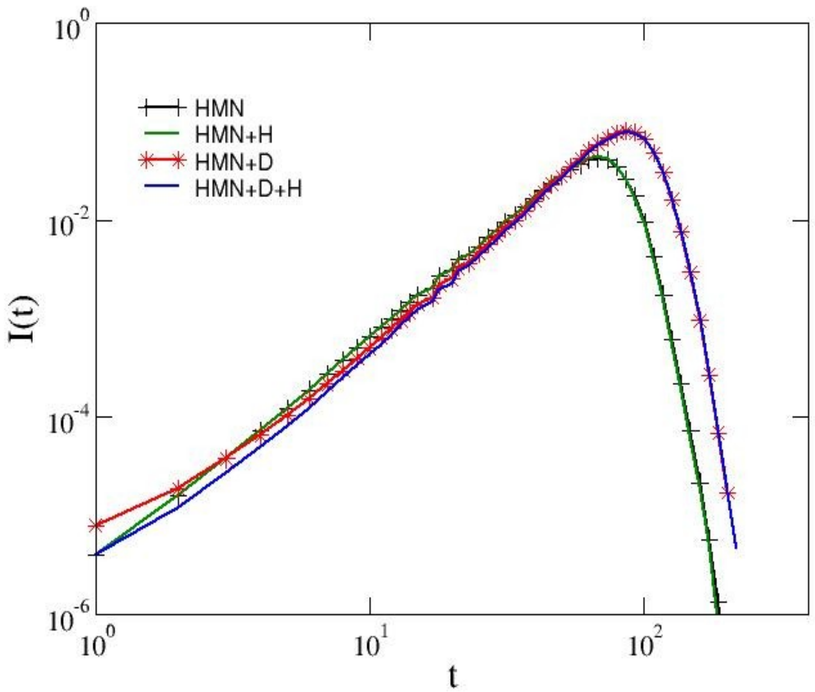

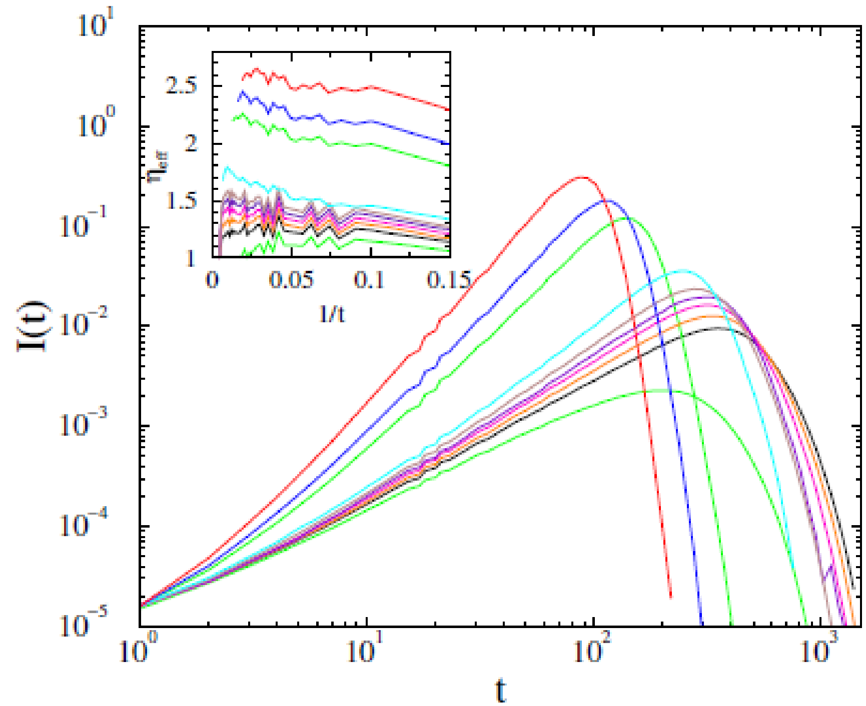

FIG. 11: The effect of a single hot-spot for the diffusive mode in graphs with $s = 4$, $b = 1$ and $\lambda = 0.22, 0.23, 0.235, 0.24$ $0.245, 0.25, 0.26, 0.4, 0.5$ (bottom to top curves). Inset: Local slopes of the same. The asymptotic critical and super critical effective exponents are roughly the same as in the non-diffusive homogeneous SIR.

Summary

TABLE I: Summary of critical SIR results for $s = 4$ HMN2d networks and Euclidean lattices. The type of graph is described by the Euclidean dimension (2d, 3d), or by the value of b for HMN2d. $+D$ denotes the diffusive case, $+H$ means the application of a single super-spreader hot-spot.

type	$\langle k \rangle$	λ_c	η	τ	d
2d	4	0.4059(1)	0.59(1)	1.06(1)	2
3d	6	0.2198(2)	0.53(2)	1.20(2)	3
2d+D	4	0.3533(1)	0.55(2)	1.058(2)	2
0.4	6.3	0.480(5)	0.8(1)	1.05(5)	2.98(2)
0.5	6.7	0.425(5)	0.95(4)	1.01(3)	3.29(1)
1.0	9.1	0.310(5)	1.4(1)	1.10(7)	3.5(1)
1.5	9.3	0.23(1)	1.30(3)	1.12(5)	3.8(1)
1.0+D	9.1	0.240(3)	1.4(1)	1.10(8)	3.5(1)
1.0+D+H	9.1	0.241(3)	1.4(1)	1.11(5)	3.5(1)

Summary

SIR SCA reproduces ***2d, 3d*** homogeneous DIP scaling behavior

TABLE I: Summary of critical SIR results for $s = 4$ HMN2d networks and Euclidean lattices. The type of graph is described by the Euclidean dimension (2d, 3d), or by the value of b for HMN2d. $+D$ denotes the diffusive case, $+H$ means the application of a single super-spreader hot-spot.

type	$\langle k \rangle$	λ_c	η	τ	d
2d	4	0.4059(1)	0.59(1)	1.06(1)	2
3d	6	0.2198(2)	0.53(2)	1.20(2)	3
2d+D	4	0.3533(1)	0.55(2)	1.058(2)	2
0.4	6.3	0.480(5)	0.8(1)	1.05(5)	2.98(2)
0.5	6.7	0.425(5)	0.95(4)	1.01(3)	3.29(1)
1.0	9.1	0.310(5)	1.4(1)	1.10(7)	3.5(1)
1.5	9.3	0.23(1)	1.30(3)	1.12(5)	3.8(1)
1.0+D	9.1	0.240(3)	1.4(1)	1.10(8)	3.5(1)
1.0+D+H	9.1	0.241(3)	1.4(1)	1.11(5)	3.5(1)

Summary

SIR SCA reproduces ***2d, 3d*** homogeneous DIP scaling behavior

With nontrivial corrections !

TABLE I: Summary of critical SIR results for $s = 4$ HMN2d networks and Euclidean lattices. The type of graph is described by the Euclidean dimension (2d, 3d), or by the value of b for HMN2d. $+D$ denotes the diffusive case, $+H$ means the application of a single super-spreader hot-spot.

type	$\langle k \rangle$	λ_c	η	τ	d
2d	4	0.4059(1)	0.59(1)	1.06(1)	2
3d	6	0.2198(2)	0.53(2)	1.20(2)	3
2d+D	4	0.3533(1)	0.55(2)	1.058(2)	2
0.4	6.3	0.480(5)	0.8(1)	1.05(5)	2.98(2)
0.5	6.7	0.425(5)	0.95(4)	1.01(3)	3.29(1)
1.0	9.1	0.310(5)	1.4(1)	1.10(7)	3.5(1)
1.5	9.3	0.23(1)	1.30(3)	1.12(5)	3.8(1)
1.0+D	9.1	0.240(3)	1.4(1)	1.10(8)	3.5(1)
1.0+D+H	9.1	0.241(3)	1.4(1)	1.11(5)	3.5(1)

Summary

SIR SCA reproduces ***2d, 3d*** homogeneous DIP scaling behavior

With nontrivial corrections !

HMN: Topology dependent scaling

TABLE I: Summary of critical SIR results for $s = 4$ HMN2d networks and Euclidean lattices. The type of graph is described by the Euclidean dimension (2d, 3d), or by the value of b for HMN2d. $+D$ denotes the diffusive case, $+H$ means the application of a single super-spreader hot-spot.

type	$\langle k \rangle$	λ_c	η	τ	d
2d	4	0.4059(1)	0.59(1)	1.06(1)	2
3d	6	0.2198(2)	0.53(2)	1.20(2)	3
2d+D	4	0.3533(1)	0.55(2)	1.058(2)	2
0.4	6.3	0.480(5)	0.8(1)	1.05(5)	2.98(2)
0.5	6.7	0.425(5)	0.95(4)	1.01(3)	3.29(1)
1.0	9.1	0.310(5)	1.4(1)	1.10(7)	3.5(1)
1.5	9.3	0.23(1)	1.30(3)	1.12(5)	3.8(1)
1.0+D	9.1	0.240(3)	1.4(1)	1.10(8)	3.5(1)
1.0+D+H	9.1	0.241(3)	1.4(1)	1.11(5)	3.5(1)

Summary

SIR SCA reproduces ***2d, 3d*** homogeneous DIP scaling behavior

With nontrivial corrections !

HMN: Topology dependent scaling

Diffusion increases epidemic sizes

but weak effect for HMN scaling

TABLE I: Summary of critical SIR results for $s = 4$ HMN2d networks and Euclidean lattices. The type of graph is described by the Euclidean dimension (2d, 3d), or by the value of b for HMN2d. $+D$ denotes the diffusive case, $+H$ means the application of a single super-spreader hot-spot.

type	$\langle k \rangle$	λ_c	η	τ	d
2d	4	0.4059(1)	0.59(1)	1.06(1)	2
3d	6	0.2198(2)	0.53(2)	1.20(2)	3
2d+D	4	0.3533(1)	0.55(2)	1.058(2)	2
0.4	6.3	0.480(5)	0.8(1)	1.05(5)	2.98(2)
0.5	6.7	0.425(5)	0.95(4)	1.01(3)	3.29(1)
1.0	9.1	0.310(5)	1.4(1)	1.10(7)	3.5(1)
1.5	9.3	0.23(1)	1.30(3)	1.12(5)	3.8(1)
1.0+D	9.1	0.240(3)	1.4(1)	1.10(8)	3.5(1)
1.0+D+H	9.1	0.241(3)	1.4(1)	1.11(5)	3.5(1)

Summary

SIR SCA reproduces ***2d, 3d*** homogeneous DIP scaling behavior

With nontrivial corrections !

HMN: Topology dependent scaling

Diffusion increases epidemic sizes

but weak effect for HMN scaling

2d growth scaling: DIP → DSIR

TABLE I: Summary of critical SIR results for $s = 4$ HMN2d networks and Euclidean lattices. The type of graph is described by the Euclidean dimension (2d, 3d), or by the value of b for HMN2d. $+D$ denotes the diffusive case, $+H$ means the application of a single super-spreader hot-spot.

type	$\langle k \rangle$	λ_c	η	τ	d
2d	4	0.4059(1)	0.59(1)	1.06(1)	2
3d	6	0.2198(2)	0.53(2)	1.20(2)	3
2d+D	4	0.3533(1)	0.55(2)	1.058(2)	2
0.4	6.3	0.480(5)	0.8(1)	1.05(5)	2.98(2)
0.5	6.7	0.425(5)	0.95(4)	1.01(3)	3.29(1)
1.0	9.1	0.310(5)	1.4(1)	1.10(7)	3.5(1)
1.5	9.3	0.23(1)	1.30(3)	1.12(5)	3.8(1)
1.0+D	9.1	0.240(3)	1.4(1)	1.10(8)	3.5(1)
1.0+D+H	9.1	0.241(3)	1.4(1)	1.11(5)	3.5(1)

Summary

SIR SCA reproduces ***2d, 3d*** homogeneous DIP scaling behavior

With nontrivial corrections !

HMN: Topology dependent scaling

Diffusion increases epidemic sizes

but weak effect for HMN scaling

2d growth scaling: DIP → DSIR

Hotspots are **ineffective**

and do not change exponents

TABLE I: Summary of critical SIR results for $s = 4$ HMN2d networks and Euclidean lattices. The type of graph is described by the Euclidean dimension (2d, 3d), or by the value of b for HMN2d. $+D$ denotes the diffusive case, $+H$ means the application of a single super-spreader hot-spot.

type	$\langle k \rangle$	λ_c	η	τ	d
2d	4	0.4059(1)	0.59(1)	1.06(1)	2
3d	6	0.2198(2)	0.53(2)	1.20(2)	3
2d+D	4	0.3533(1)	0.55(2)	1.058(2)	2
0.4	6.3	0.480(5)	0.8(1)	1.05(5)	2.98(2)
0.5	6.7	0.425(5)	0.95(4)	1.01(3)	3.29(1)
1.0	9.1	0.310(5)	1.4(1)	1.10(7)	3.5(1)
1.5	9.3	0.23(1)	1.30(3)	1.12(5)	3.8(1)
1.0+D	9.1	0.240(3)	1.4(1)	1.10(8)	3.5(1)
1.0+D+H	9.1	0.241(3)	1.4(1)	1.11(5)	3.5(1)

Summary

SIR SCA reproduces ***2d, 3d*** homogeneous DIP scaling behavior

With nontrivial corrections !

HMN: Topology dependent scaling

Diffusion increases epidemic sizes

but weak effect for HMN scaling

2d growth scaling: DIP → DSIR

Hotspots are **ineffective**

and do not change exponents

TABLE I: Summary of critical SIR results for $s = 4$ HMN2d networks and Euclidean lattices. The type of graph is described by the Euclidean dimension (2d, 3d), or by the value of b for HMN2d. $+D$ denotes the diffusive case, $+H$ means the application of a single super-spreader hot-spot.

type	$\langle k \rangle$	λ_c	η	τ	d
2d	4	0.4059(1)	0.59(1)	1.06(1)	2
3d	6	0.2198(2)	0.53(2)	1.20(2)	3
2d+D	4	0.3533(1)	0.55(2)	1.058(2)	2
0.4	6.3	0.480(5)	0.8(1)	1.05(5)	2.98(2)
0.5	6.7	0.425(5)	0.95(4)	1.01(3)	3.29(1)
1.0	9.1	0.310(5)	1.4(1)	1.10(7)	3.5(1)
1.5	9.3	0.23(1)	1.30(3)	1.12(5)	3.8(1)
1.0+D	9.1	0.240(3)	1.4(1)	1.10(8)	3.5(1)
1.0+D+H	9.1	0.241(3)	1.4(1)	1.11(5)	3.5(1)

Quenched disorder in rates is irrelevant for SIR!

Summary

SIR SCA reproduces ***2d, 3d*** homogeneous DIP scaling behavior

With nontrivial corrections !

HMN: Topology dependent scaling

Diffusion increases epidemic sizes

but weak effect for HMN scaling

2d growth scaling: DIP → DSIR

Hotspots are **ineffective**

and do not change exponents

PL decay of *I(t)* in herd immunity regime is not observed !

TABLE I: Summary of critical SIR results for $s = 4$ HMN2d networks and Euclidean lattices. The type of graph is described by the Euclidean dimension (2d, 3d), or by the value of b for HMN2d. $+D$ denotes the diffusive case, $+H$ means the application of a single super-spreader hot-spot.

type	$\langle k \rangle$	λ_c	η	τ	d
2d	4	0.4059(1)	0.59(1)	1.06(1)	2
3d	6	0.2198(2)	0.53(2)	1.20(2)	3
2d+D	4	0.3533(1)	0.55(2)	1.058(2)	2
0.4	6.3	0.480(5)	0.8(1)	1.05(5)	2.98(2)
0.5	6.7	0.425(5)	0.95(4)	1.01(3)	3.29(1)
1.0	9.1	0.310(5)	1.4(1)	1.10(7)	3.5(1)
1.5	9.3	0.23(1)	1.30(3)	1.12(5)	3.8(1)
1.0+D	9.1	0.240(3)	1.4(1)	1.10(8)	3.5(1)
1.0+D+H	9.1	0.241(3)	1.4(1)	1.11(5)	3.5(1)

Quenched disorder in rates is irrelevant for SIR!

Summary

SIR SCA reproduces ***2d, 3d*** homogeneous DIP scaling behavior

With nontrivial corrections !

HMN: Topology dependent scaling

Diffusion increases epidemic sizes

but weak effect for HMN scaling

2d growth scaling: DIP → DSIR

Hotspots are **ineffective**

and do not change exponents

TABLE I: Summary of critical SIR results for $s = 4$ HMN2d networks and Euclidean lattices. The type of graph is described by the Euclidean dimension (2d, 3d), or by the value of b for HMN2d. $+D$ denotes the diffusive case, $+H$ means the application of a single super-spreader hot-spot.

type	$\langle k\rangle$	λ_c	η	τ	d
2d	4	0.4059(1)	0.59(1)	1.06(1)	2
3d	6	0.2198(2)	0.53(2)	1.20(2)	3
2d+D	4	0.3533(1)	0.55(2)	1.058(2)	2
0.4	6.3	0.480(5)	0.8(1)	1.05(5)	2.98(2)
0.5	6.7	0.425(5)	0.95(4)	1.01(3)	3.29(1)
1.0	9.1	0.310(5)	1.4(1)	1.10(7)	3.5(1)
1.5	9.3	0.23(1)	1.30(3)	1.12(5)	3.8(1)
1.0+D	9.1	0.240(3)	1.4(1)	1.10(8)	3.5(1)
1.0+D+H	9.1	0.241(3)	1.4(1)	1.11(5)	3.5(1)

PL decay of *I(t)* in herd immunity regime is not observed !

G. Ó. : *PRE 103 (2021) 062112*, S.D. G.Ó. *Phys. Rev. E 107 (2023) 014303*

Quenched disorder in rates is irrelevant for SIR!

OTKA K128989 and NIIF supercomputer network support

SIR Modelling

SIR Modelling

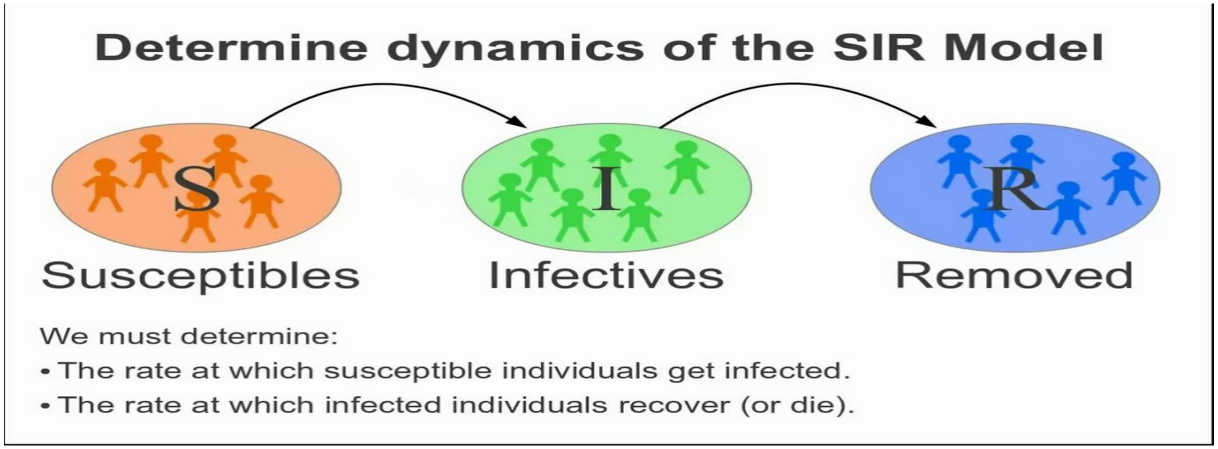

SIR Modelling

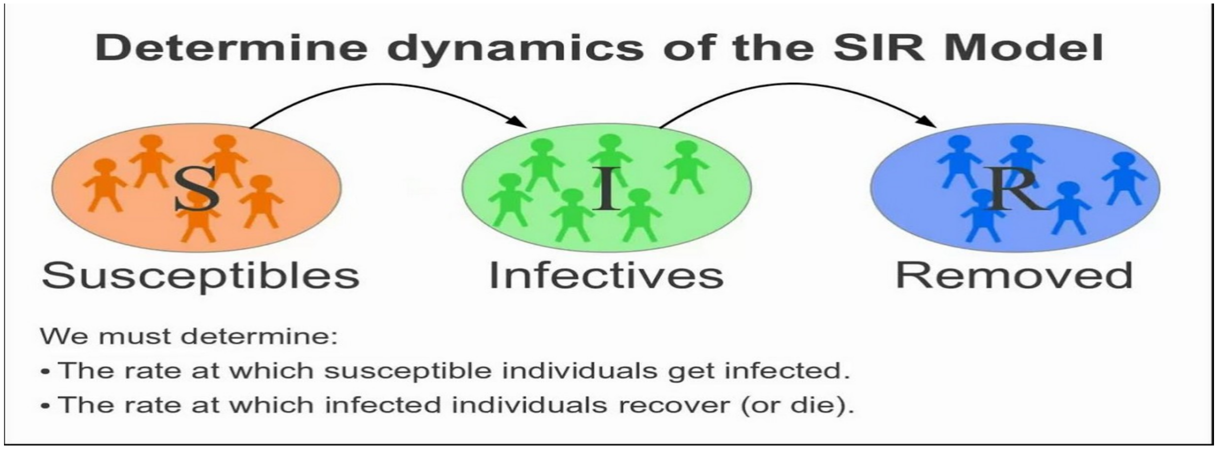

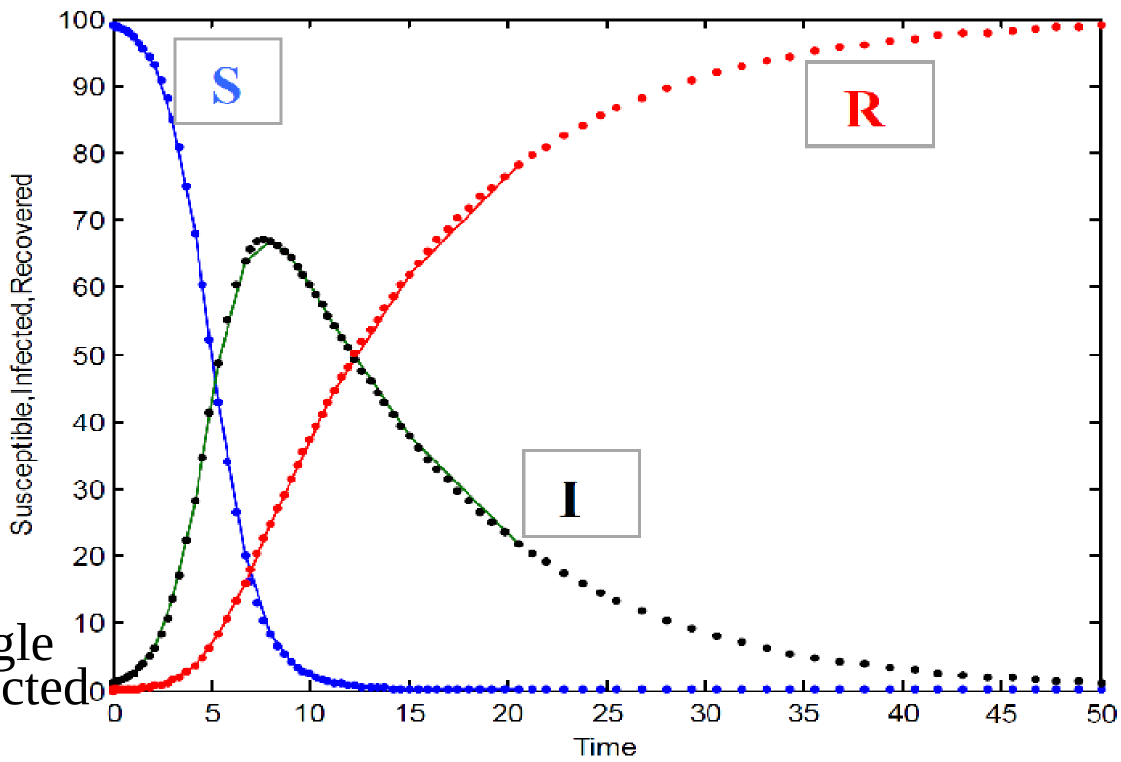

Single infected

SIR Modelling

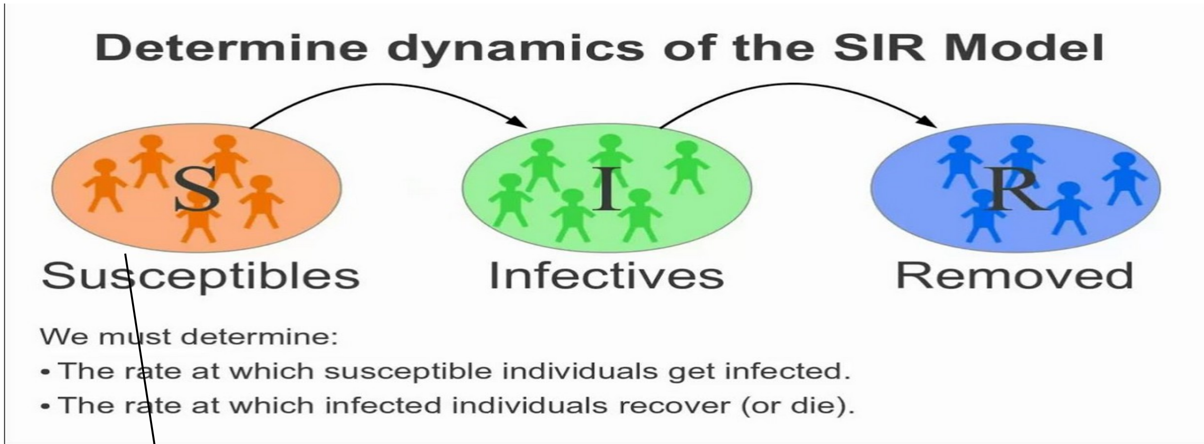

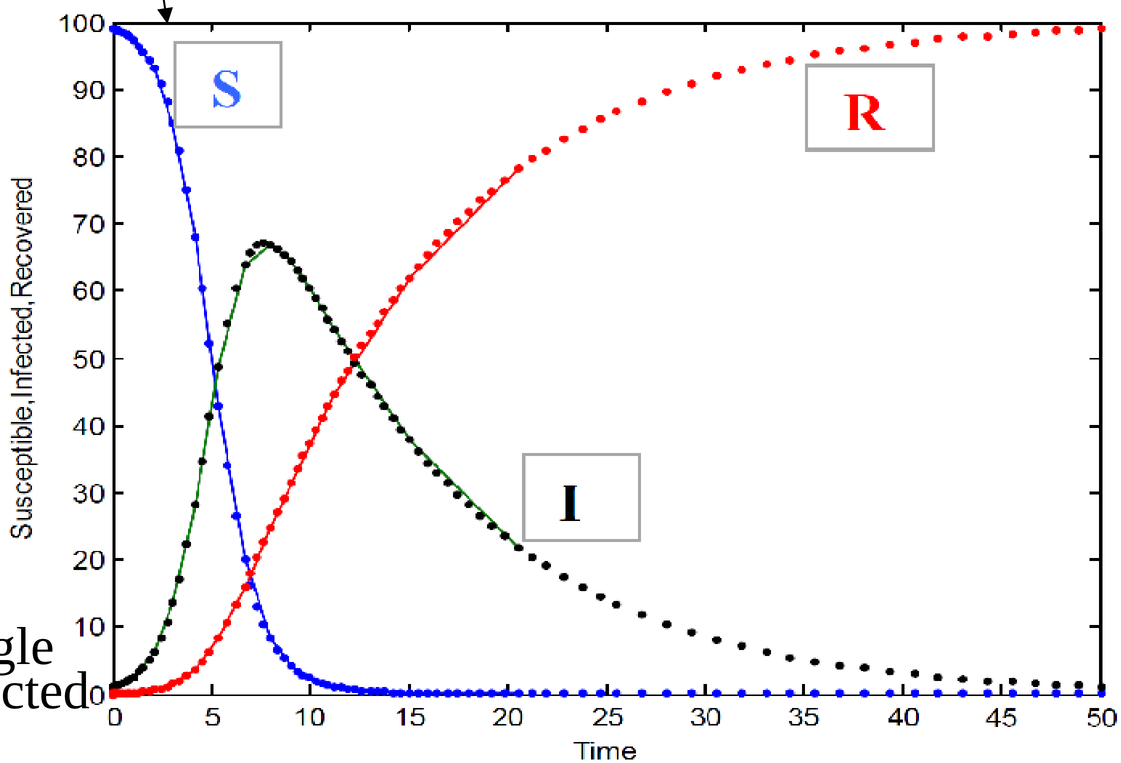

Single infected

SIR Modelling

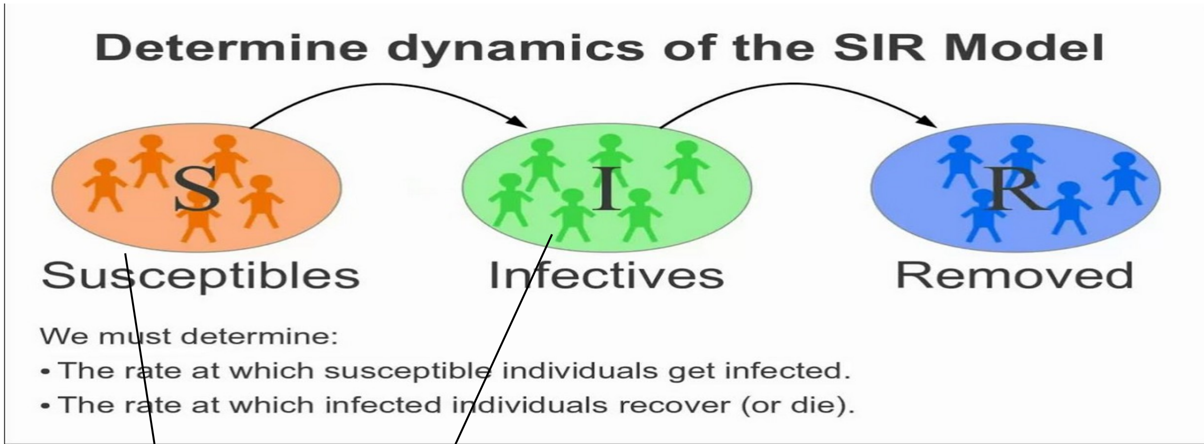

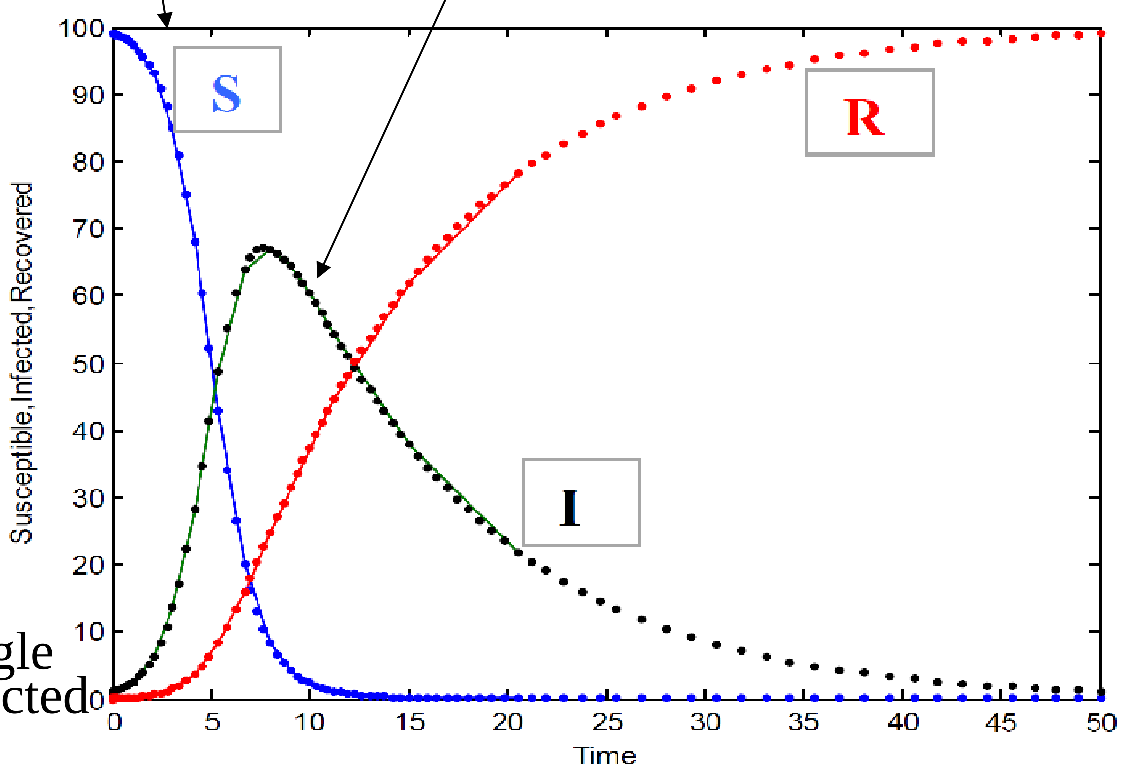

Single infected

SIR Modelling

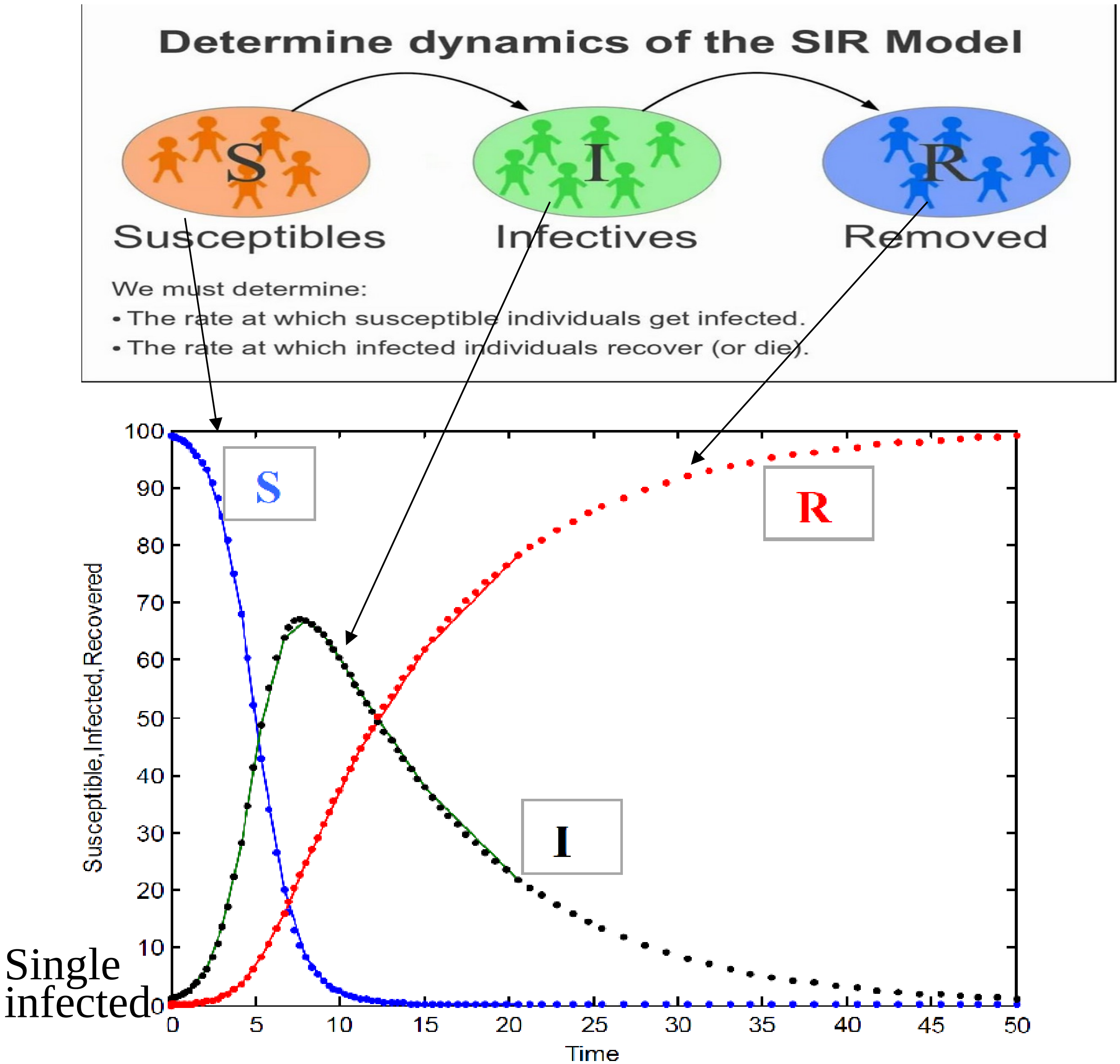

SIR Modelling

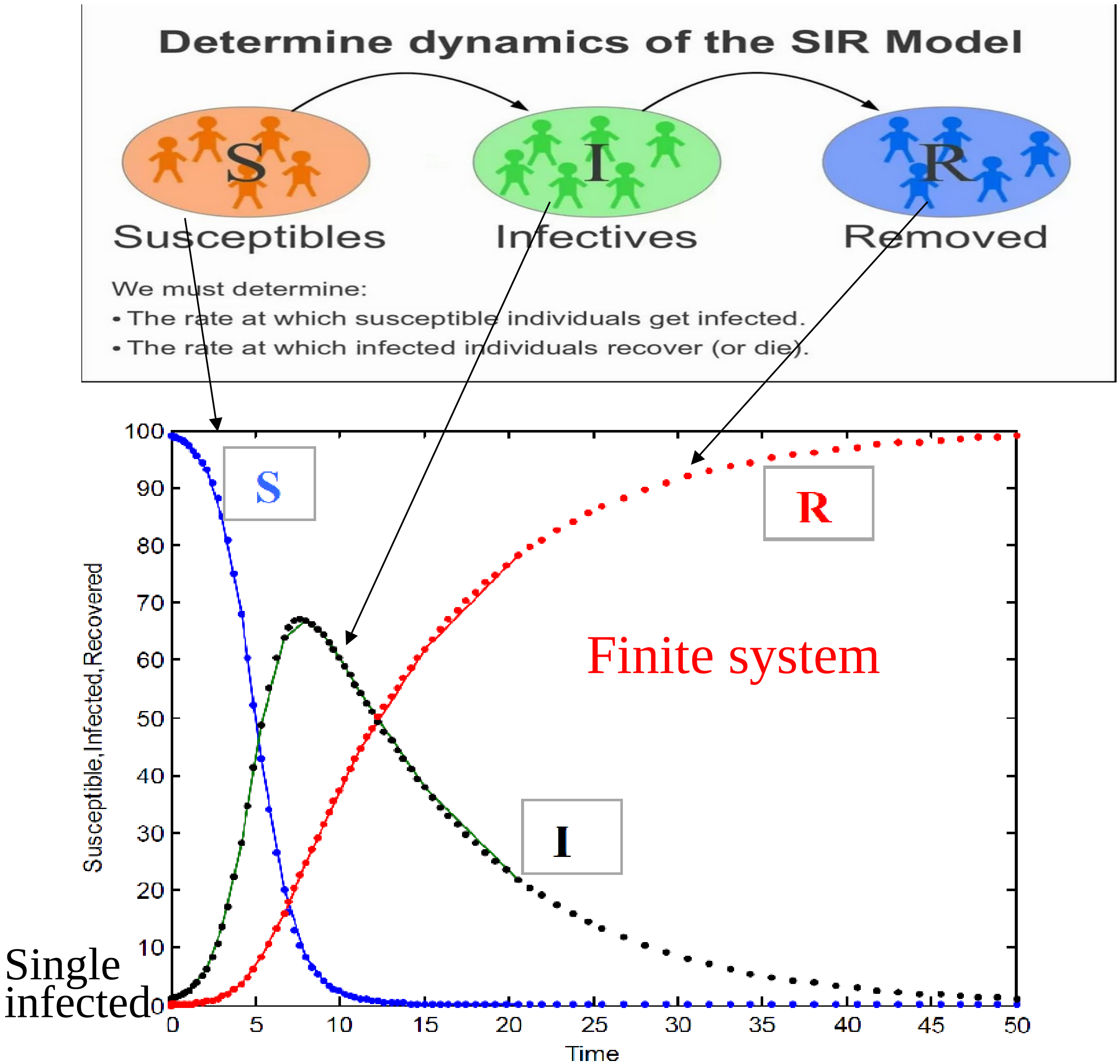

SIR Modelling

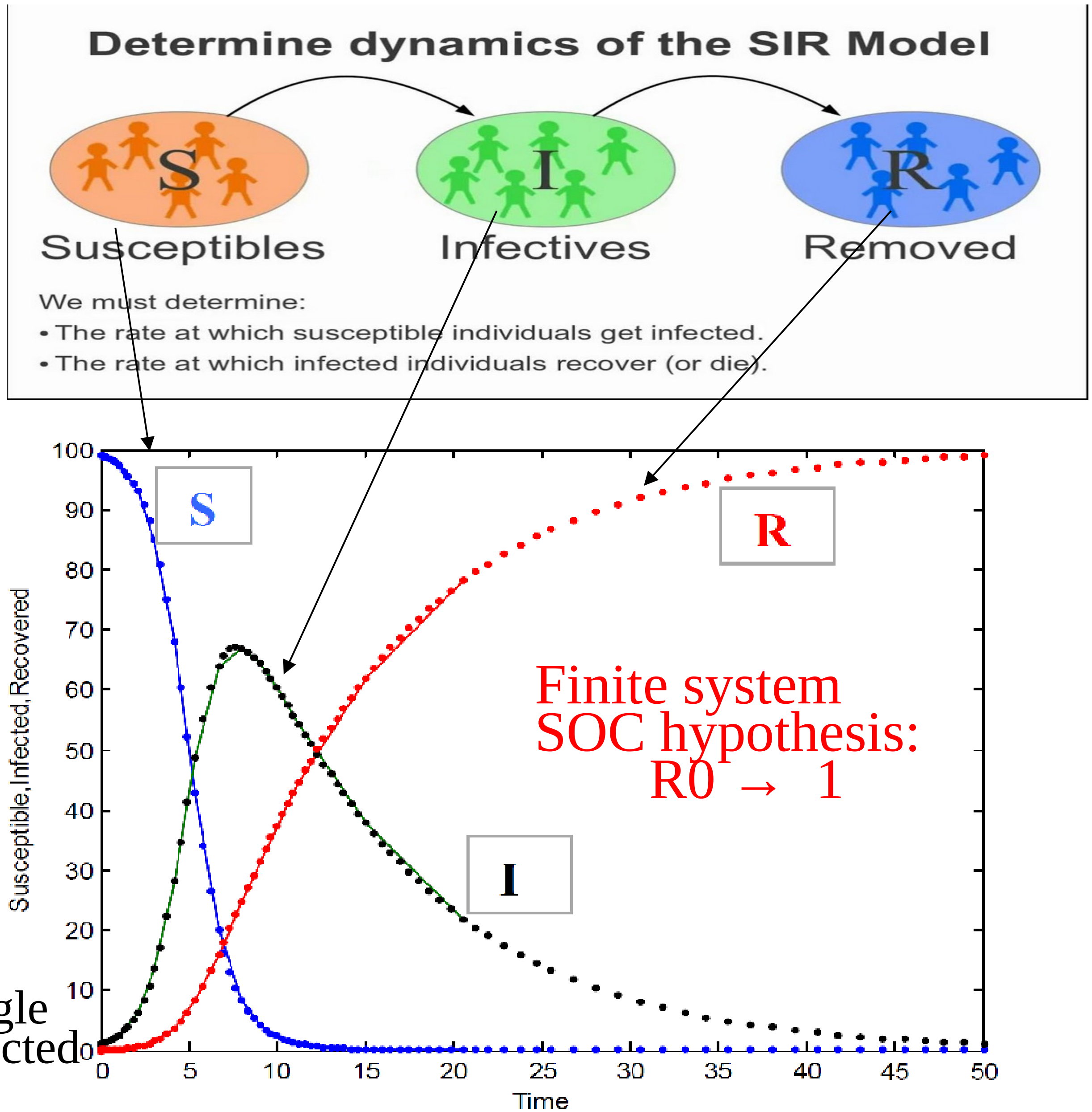

Finite system
SOC hypothesis:
R0 → 1

Single
infected

SIR Modelling

At the critical point:

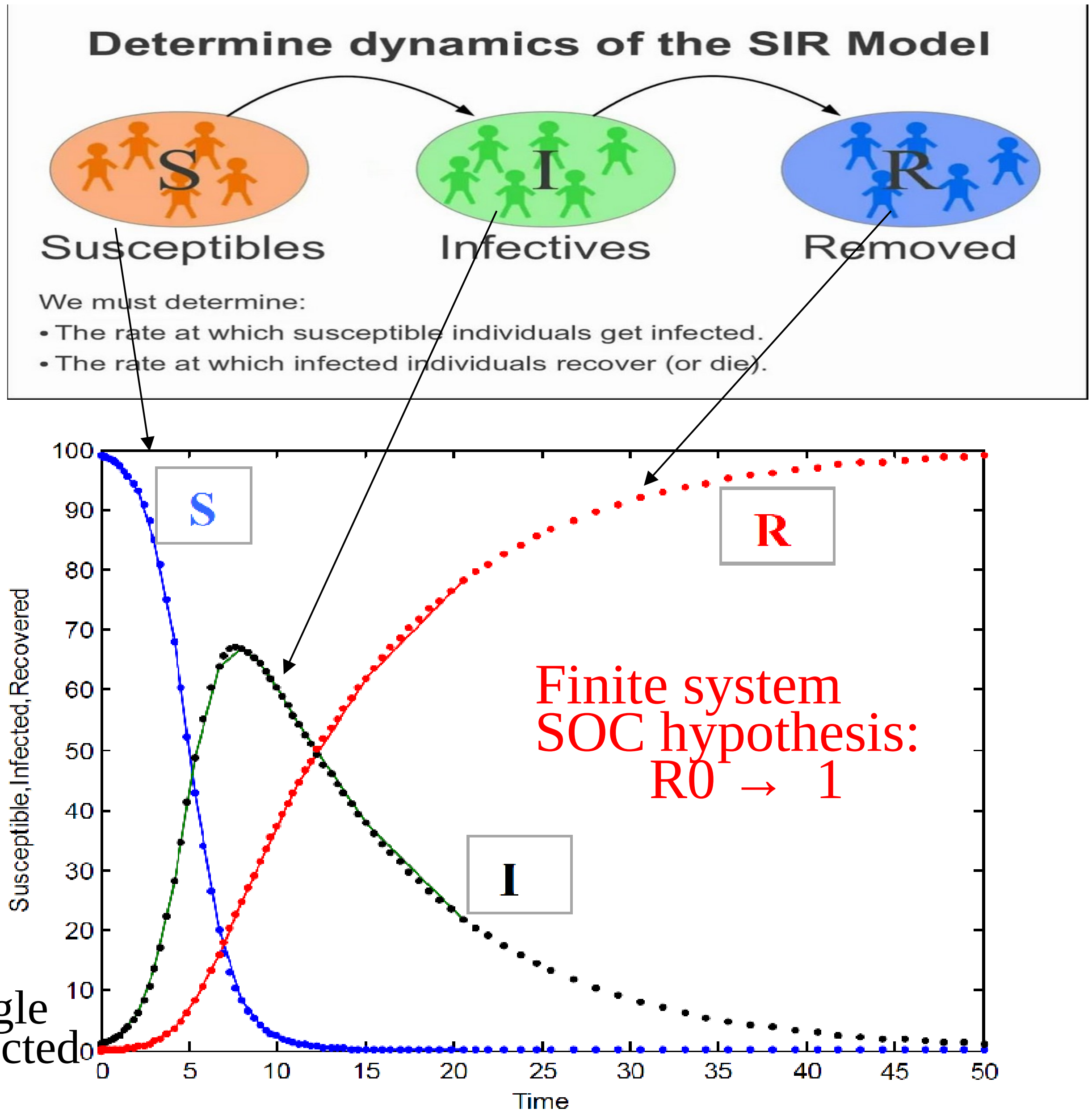

Single infected

SIR Modelling

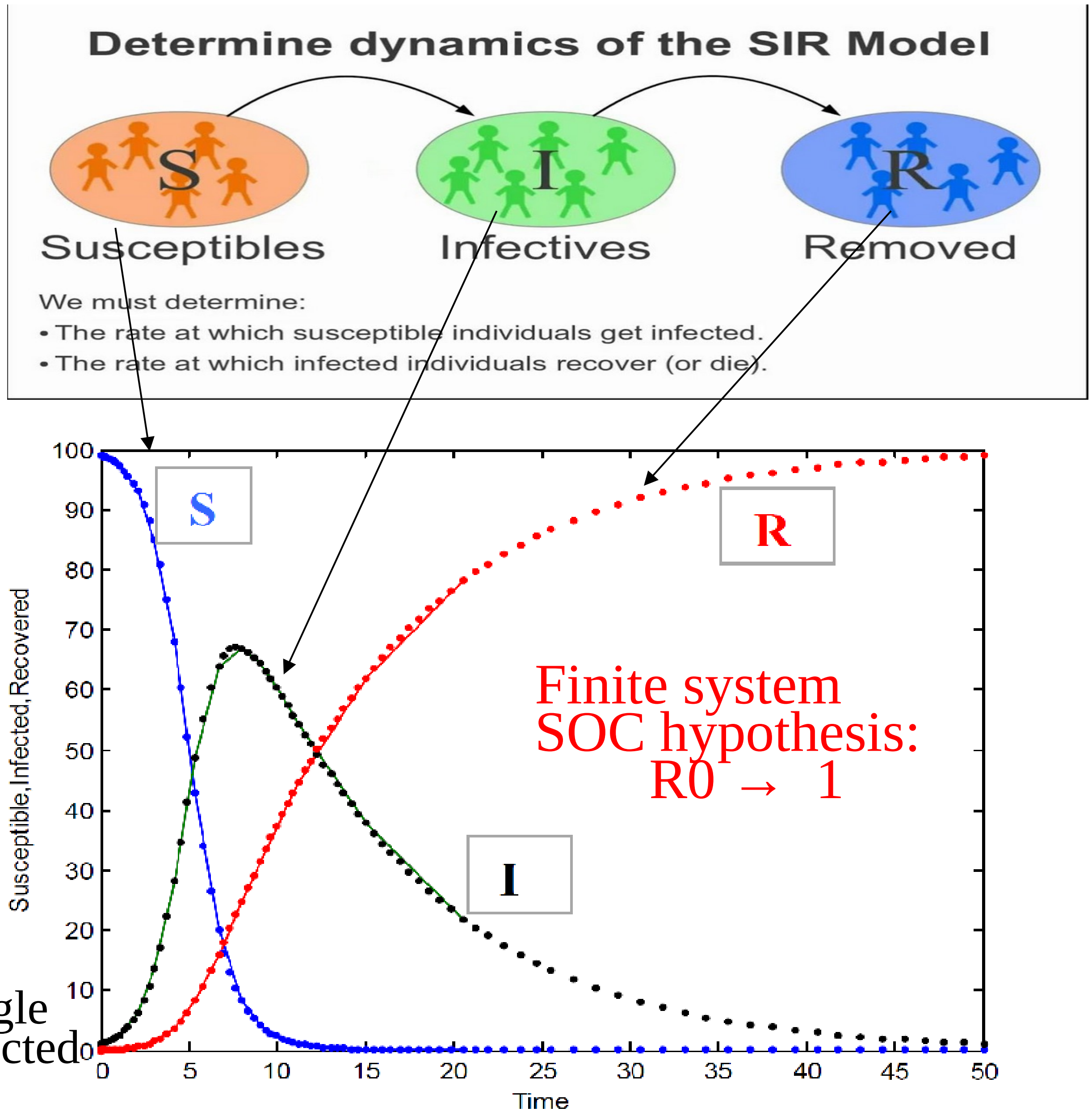

Single infected

At the critical point:

Dynamical **I**sotropic **P**ercolation Universality (**DIP**) class

scaling behavior

SIR Modelling

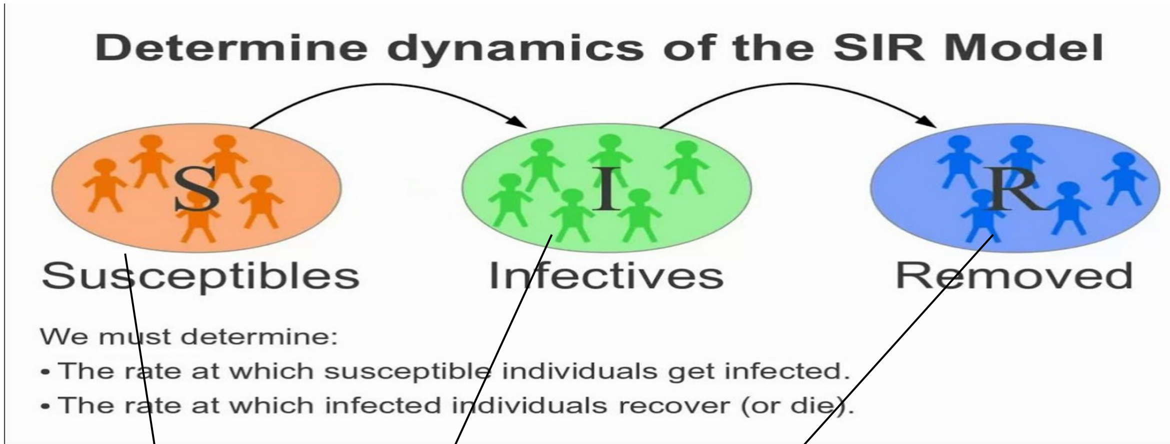

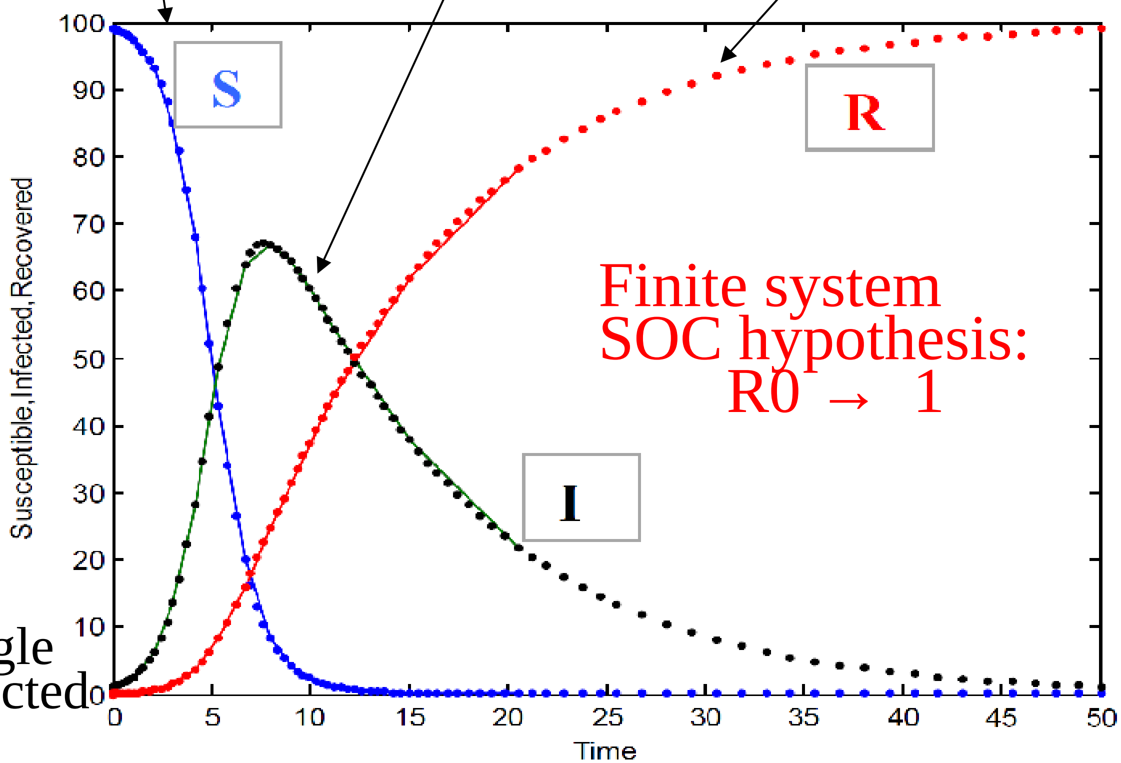

Single infected

At the critical point:

Dynamical **I**sotropic Universality (**DIP**) class

scaling behavior

TABLE II. Critical exponents for dynamical percolation. Exponents calculated by using scaling relations contained in this paper are reported in the lower part. The rest of the exponent values are from [37]. Where not reported uncertainties are in the last digit. For $d=2$, values expressed as fractions refer to exact results [37]. For $d=6$ we report the exact mean field values.

Exponent	$d=2$	$d=3$	$d=6$
$\beta=\beta'$	5/36	0.417	1
$\nu_{\|\|}$	1.506	1.169	1
γ	43/18	1.795	1
$\nu_{\perp}$	4/3	0.875	1/2
τ	96/91	1.188	3/2
σ	36/91	0.452	1/2
D_f	91/48	2.528	4
τ_t	1.092	1.356	2
σ_t	0.664	0.855	1
γ_t	1.367	0.752	0
η	0.586	0.536	0
$\delta=\theta$	0.092	0.356	1
z	1.771	1.497	1

SIR Modelling

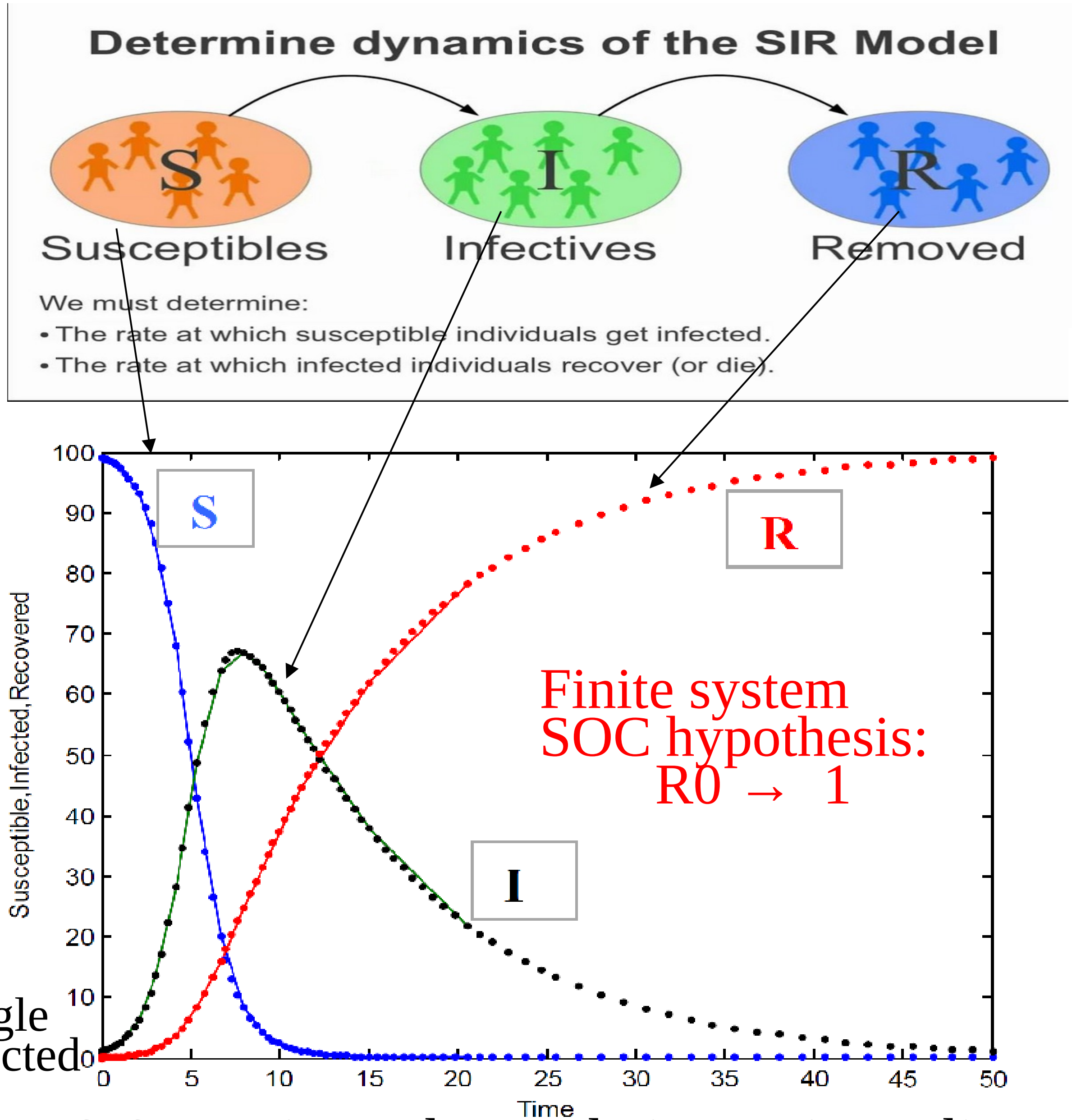

Single infected

SIS → **D**irected **P**ercolation Universality

At the critical point:

Dynamical **I**sotropic Universality (**DIP**) class

scaling behavior

TABLE II. Critical exponents for dynamical percolation. Exponents calculated by using scaling relations contained in this paper are reported in the lower part. The rest of the exponent values are from [37]. Where not reported uncertainties are in the last digit. For $d=2$, values expressed as fractions refer to exact results [37]. For $d=6$ we report the exact mean field values.

Exponent	$d=2$	$d=3$	$d=6$
$\beta=\beta'$	5/36	0.417	1
$\nu_{\parallel}$	1.506	1.169	1
γ	43/18	1.795	1
$\nu_{\perp}$	4/3	0.875	1/2
τ	96/91	1.188	3/2
σ	36/91	0.452	1/2
D_f	91/48	2.528	4
τ_t	1.092	1.356	2
σ_t	0.664	0.855	1
γ_t	1.367	0.752	0
η	0.586	0.536	0
$\delta=\theta$	0.092	0.356	1
z	1.771	1.497	1

Power-law distribution in the number of confirmed COVID-19 cases

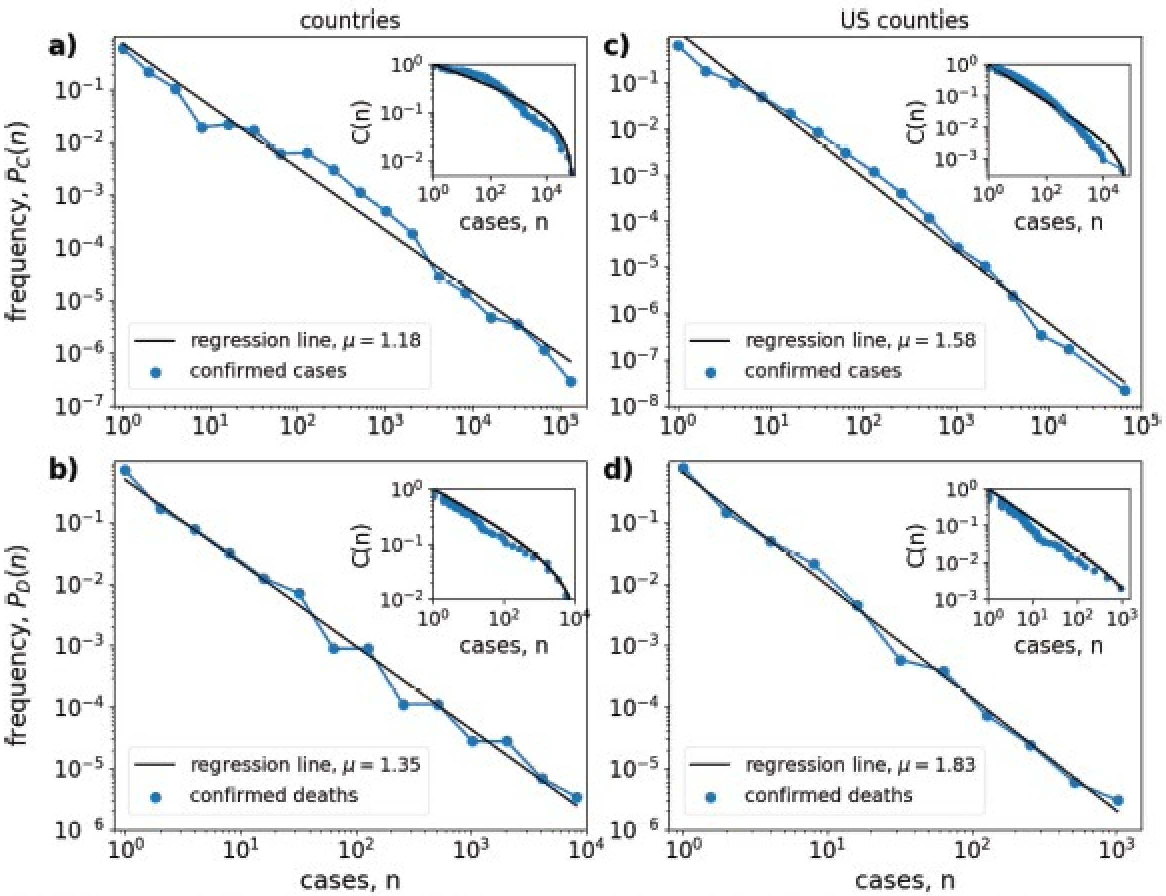

FIG. 1. Power-law scaling in the distribution of confirmed COVID-19 cases. Left column: Estimated probability $P_x(n)$ (blue lines and circles) for a country to have a certain number n of (a) confirmed cases ($x = C$) and (b) confirmed deaths ($x = D$) on March 22, 2020. Right column: The same for the 2160 US counties that have been invaded by the coronavirus on March 31, 2020. Histogram bins are spaced equally on a logarithmic axis and only bins with a positive number of entries are shown. Black solid lines show straight-line fits with slope μ, indicated in the figure labels. Insets: Cumulative fraction $C(n) = \sum_{m=n+1}^{N} P(m)$ of countries, or counties, with case number $m > n$. Solid lines show the cumulative distribution equation (A2) of a truncated power-law distribution with critical exponent μ and cut-off value (a) $n_{max} = 1 \times 10^5$, (b) $n_{max} = 1.5 \times 10^4$, (c) $n_{max} = 7 \times 10^4$, and (d) $n_{max} = 3 \times 10^3$.

B. Blausius: Chaos 30, 093123 (2020); doi: 10.1063/5.0013031